diversity

MDPI

Article

Deep-Sea Tardigrades from the North-Western Pacific, with Descriptions of Two New Species

Anastasiia A. Saulenko [1,*], Anastassya S. Maiorova [2], Pedro Martínez Arbizu [3] and Vladimir V. Mordukhovich [1,2,*]

[1] Department of Marine Ecology, Far Eastern Federal University, 690922 Vladivostok, Russia
[2] A.V. Zhirmunsky National Scientific Center of Marine Biology, Far Eastern Branch, Russian Academy of Sciences, 690041 Vladivostok, Russia
[3] German Center for Marine Biodiversity Research (DZMB), Senckenberg am Meer, Südstrand 44, 26382 Wilhelmshaven, Germany
* Correspondence: saulenko.aa@mail.ru (A.A.S.); vvmora@mail.ru (V.V.M.)

Abstract: Three deep-sea tardigrade species were identified from the sediment samples collected during the four German–Russian joint deep-sea cruises that were conducted in the North-Western Pacific: *Coronarctus sonne* sp. nov., *Moebjergarctus okhotensis* sp. nov., and *Angursa* cf. *bicuspis*. Specimens of those species were collected at depths between 1700 and 5410 m. The new species *Coronarctus sonne* sp. nov. belongs to the *Cor. tenellus* group of species on the basis of morphological traits such as the short cephalic appendages and heteromorphic claws. The structure of the secondary clavae and two points, with an accessory point and a primary point simultaneously on the internal and external claws on legs IV, are significant characteristics distinguishing *Coronarctus sonne* sp. nov. from other described species. *Moebjergarctus okhotensis* sp. nov. is characterized by having cephalic cirri with the long smooth portion of the scapus and annulated scapus only in the basal portion, the structure of the male and female reproductive system, and differences in the sizes of some structures compared to the other described species. An analysis of the results of four deep-sea expeditions indicates a patchy distribution of tardigrades in the North-Western Pacific.

Keywords: meiofauna; tardigrade; taxonomy; *Coronarctus*; *Moebjergarctus*; *Angursa*; deep sea; the North-Western Pacific

Citation: Saulenko, A.A.; Maiorova, A.S.; Martínez Arbizu, P.; Mordukhovich, V.V. Deep-Sea Tardigrades from the North-Western Pacific, with Descriptions of Two New Species. *Diversity* **2022**, *14*, 1086. https://doi.org/10.3390/d14121086

Academic Editors: Elena S. Chertoprud and Daniel Stec

Received: 30 September 2022
Accepted: 4 December 2022
Published: 8 December 2022

1. Introduction

Tardigrades are a type of hydrophilic micrometazoans with four pairs of lobopodous legs. They are ubiquitous in terrestrial, freshwater, and marine ecosystems [1]. Despite their microscopic size, they display complex morphological and anatomical structures, and many are known for their ability to tolerate extreme environmental conditions [2]. More than 1400 species of tardigrades from miscellaneous habitats have been described so far [3], but it is estimated that the total global number of tardigrades will be an order of magnitude higher [4].

Marine tardigrades are found in a variety of marine habitats, from the intertidal areas down to the hadal zone (ultra-abyss) [1,5,6]. They inhabit various types of bottom sediments, occurring in silts, coarse-grained sand, on rocks and algae, and sometimes on other invertebrates as commensals and ectoparasites [1,5,7]. However, despite their wide occurrence, knowledge on the diversity and spatial distribution of marine tardigrades remains scarce. Marine tardigrades, as a rule, require special and laborious methods of collection and examination. The morphology-based identification of species requires a lot of time and high qualifications. Moreover, it is often impossible to identify specimens to the exact species based only on morphological characteristics [8]. At the same time, the use of genetic data is also often limited due to the insufficient number of samples of many species or the lack of suitable primers. This greatly complicates the study of the

biodiversity and taxonomy of marine tardigrades [9]. Over 230 tardigrade species have been described to date from marine habitats (mostly intertidal), which is estimated to represent approximately 16% of all valid species [3,5]. Bartels et al. [9] suggested that the actual number of marine tardigrade species may be higher than that of the carefully studied terrestrial and freshwater representatives.

The lack of information on marine tardigrades of the deep-sea communities is most evident. Deep-sea species (reported deeper than 200 m) make up only ca. 20 percent of the known diversity of marine tardigrades [5,10–13]. Data on tardigrade fauna are almost absent in some regions of the world ocean. Thus, only one species is known from the deep-sea ecosystems of the North-Western Pacific Ocean (NWPO): *Angursa seisuimaruae* Fujimoto and Hansen, 2019 [14]. However, tardigrades are recorded in the deep-sea meiofauna of this region [6,15]. During four German–Russian deep-sea cruises to the NWPO [16], tardigrades were noted at 23 stations among 46 (Figure 1, Table 1). Three species of tardigrades, two of which were new to science, were found in bottom sediments sampled on these cruises.

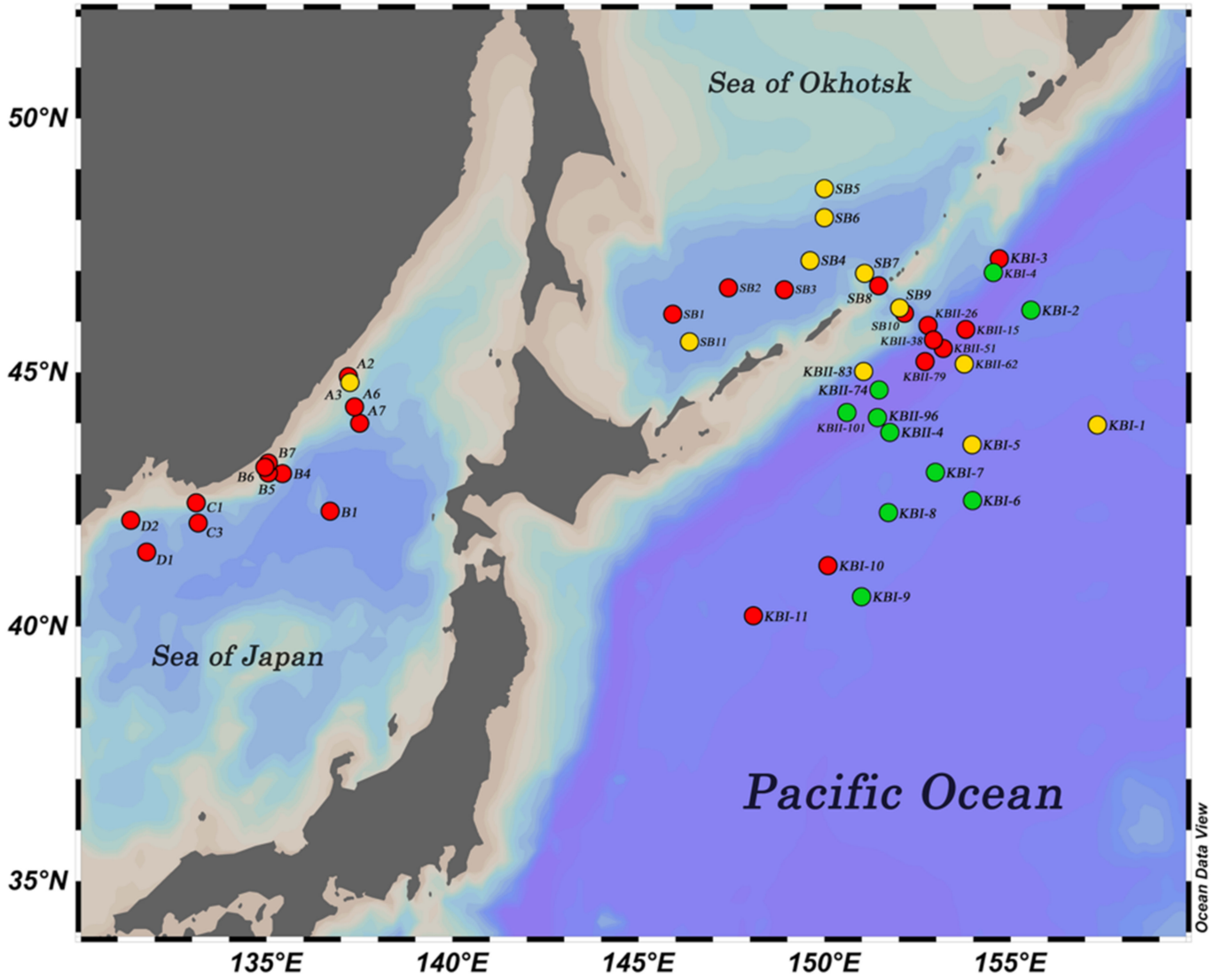

Figure 1. Map of the sampling area of four joint German–Russian deep-sea research cruises (green dots—stations where tardigrades were found; yellow dots—stations where tardigrades were identified; red dots—stations where tardigrades were not found).

Table 1. Information about stations where tardigrades were found (?—not studied).

Cruise (Year)	Station	Latitude, N	Longitude, E	Depth, m	Mean Abundance (ind./10 cm^2)	References	Species
SoJaBio 2010	A3	44.80	137.25	1473	0.03	This study	*Angursa* sp.
SokhoBio 2015	SB4	47.20 48.62	149.62 150.00	3366	0.08	This study This study	*Moebjergarctus okhotensis* sp. nov. *Angursa* cf. *bicuspis*
SokhoBio 2015	SB5	48.05	150.00	1700	0.3	This study	*Angursa* cf. *bicuspis*
SokhoBio 2015	SB6	46.95 46.27	151.08 152.03	3351	1.23	This study This study	*Moebjergarctus okhotensis* sp. nov. *Angursa* cf. *bicuspis*
SokhoBio 2015	SB7	45.60	146.38	3300	1.31	This study	*Angursa* cf. *bicuspis*
SokhoBio 2015	SB9	43.97	157.33	3342	0.04	This study	*Angursa* cf. *bicuspis*
SokhoBio 2015	SB11	46.23	155.55	3206	1.52	This study	*Angursa* cf. *bicuspis*
KuramBio I (2012)	KBI-1	46.97	154.54	5410	1.16	Schmidt and Martinez Arbizu, 2015 [15]	*Coronarctus sonne* sp. nov.
KuramBio I (2012)	KBI-2	43.58	153.97	4869	0.02	Schmidt and Martinez Arbizu, 2015 [15]	?
KuramBio I (2012)	KBI-4	42.48	153.99	4972	0.14	Schmidt and Martinez Arbizu, 2015 [15]	?
KuramBio I (2012)	KBI-5	43.04	152.99	5378	1.27	Schmidt and Martinez Arbizu, 2015 [15]	*Coronarctus sonne* sp. nov.
KuramBio I (2012)	KBI-6	42.24	151.73	5298	0.05	Schmidt and Martinez Arbizu, 2015 [15]	?
KuramBio I (2012)	KBI-7	40.58	151.00	5221	0.02	Schmidt and Martinez Arbizu, 2015 [15]	?
KuramBio I (2012)	KBI-8	43.82	151.76	5128	0.02	Schmidt and Martinez Arbizu, 2015 [15]	?
KuramBio I (2012)	KBI-9	45.17	153.76	5406	0.02	Schmidt and Martinez Arbizu, 2015 [15]	?
KuramBio II (2016)	KBII-4	44.66	151.47	5143	0.28	Schmidt et al., 2019 [6]	?
KuramBio II (2016)	KBII-62	45.02	151.05	5743	0.28	Schmidt et al., 2019 [6]	*Angursa* sp.
KuramBio II (2016)	KBII-74	44.11	150.60	8226	0.05	Schmidt et al., 2019 [6]	?
KuramBio II (2016)	KBII-83	44.21	150.60	5212	0.05	Schmidt et al., 2019 [6]	*Angursa* sp.
KuramBio II (2016)	KBII-96	44.80	137.25	6515	0.42	Schmidt et al., 2019 [6]	?
KuramBio II (2016)	KBII-101	47.20	149.62	9540	0.24	Schmidt et al., 2019 [6]	?

2. Material and Methods

Tardigrades were extracted from sediment samples collected during the four German–Russian joint deep-sea cruises that were conducted in the North-Western Pacific in 2010, 2012, 2015, and 2016 (SoJaBio (2010), KuramBio I (2012), SokhoBio (2015), and KuramBio II (2016)). The study area included the Sea of Japan, the Sea of Okhotsk, and the Pacific Ocean.

In the SoJaBio, KuramBio I, and KuramBio II expeditions, sediments were sampled with a multicorer (diameter: 10 cm). In the SokhoBio expedition, samples were taken with a plastic tube (diameter: 10 cm) from bottom sediments collected by a box corer (capture area: 0.25 m^2). For meiofauna investigations, the upper 5 cm of the sediment cores were fixed in 4% buffered formaldehyde. In the laboratory, samples from all cruises were processed identically. Sediments were washed with tap water, passed through a 32 µm sieve, and centrifuged in a solution of kaolin/colloidal silica three times (4000 rpm for 6 min) [17]. Afterwards, the meiofauna samples were refixed in formalin and stained with rose bengal. Tardigrades were collected using stereomicroscopes, transferred by a fine tungsten wire needle and Irwin loop, and mounted in VECTASHIELD® mounting medium between two slips in plastic Higgins–Shiroyama slides (cover glasses 22 and 18 mm in length sealed by transparent nail polish), which enabled viewing from both sides.

In general, tardigrades were studied from 11 stations (Table 1). Drawings and photographs were made on an Olympus BX 53 optical microscope using differential interference contrast (DIC) microscopy. The morphological structures were measured only if they were

undamaged and if their orientation was suitable. For scanning electron microscopy, selected specimens were transferred from 4% formaldehyde to a vessel of distilled water and washed using a detergent to clean the body surface. The cleaned specimens were dehydrated through a graded series of ethanol (30–50–70–90–96% (I)–96% (II) with 15′ in each solution), transferred to acetone (10′ in each solution), and critical-point-dried. The dried specimens were mounted on aluminum stubs, coated with gold, and observed using a Zeiss® Sigma 300 VP scanning electron microscope.

Tardigrade taxonomy followed Guil et al., 2019 [18], and Degma et al., 2009–2022 [3], and morphological terminology followed Møbjerg et al., 2018 [19]. The identification and differentiation of the new species were conducted using the key by Gomes-Júnior et al., 2019 [12], for the genus *Coronarctus*; the key by Fujimoto and Hansen, 2019 [10], for the genus *Angursa;* and the original descriptions of all valid species of genera *Angursa*, *Coronarctus,* and *Moebjergarctus*. Abbreviations for the names of genera are given according to Perry et al., 2019 [20].

3. Results

3.1. Taxonomy

Phylum Tardigrada Doyère, 1840
Class Heterotardigrada Marcus, 1927
Order Arthrotardigrada Marcus, 1927
Family: Coronarctidae Renaud-Mornant, 1974
Genus: *Coronarctus* Renaud-Mornant, 1974
Coronarctus sonne sp. nov.
(Figures 2–10, Table 2)
urn: lsid: zoobank.org: act:8D49211B-86DE-42D4-AFBA-6C64F6A08F85

Table 2. Body measurements (in µm) of *Coronarctus sonne* sp. nov. type series. Body width was measured between legs III and IV; ?—trait not measurable.

Character	Holotype, Male	Paratype, Male	Paratype, Female
Body length	494	542	557
Body width	104	134	113
Internal cirri	9.6	8.7	6.9
External cirri	10.1	9.3	10.4
Median cirrus	5.3	5.3	4.2
Primary clava	8.7	8.4	9.4
Cirri *A*	8.6	6.3	7.3
Cirri *B*	7.0	7.0	7.1
Cirri *C*	38.0	21.3	22.7
Cirri *E*	36.3	32.7	30.2
Sensory organ on leg I	6.3	?	9.9
Sensory organ on leg II	8.4	9.9	7.8
Sensory organ on leg III	9.1	9.3	?
Sensory organ on leg IV	19.1	16.9	15.1
Process on leg IV	15.3	17.6	14.1
Leg I: Claw I	26.2	25.6	20.6
Claw II	36.8	33.0	26.3
Claw III	32.1	30.3	?
Claw IV	26.4	24.0	?
Leg IV: Claw I	48.3	44.2	49.2
Claw II	55.7	67.6	64.0
Claw III	56.5	58.0	68.5
Claw IV	45.1	49.6	51.3
Gonopore–anus (distance)	16.9	15.4	22.5

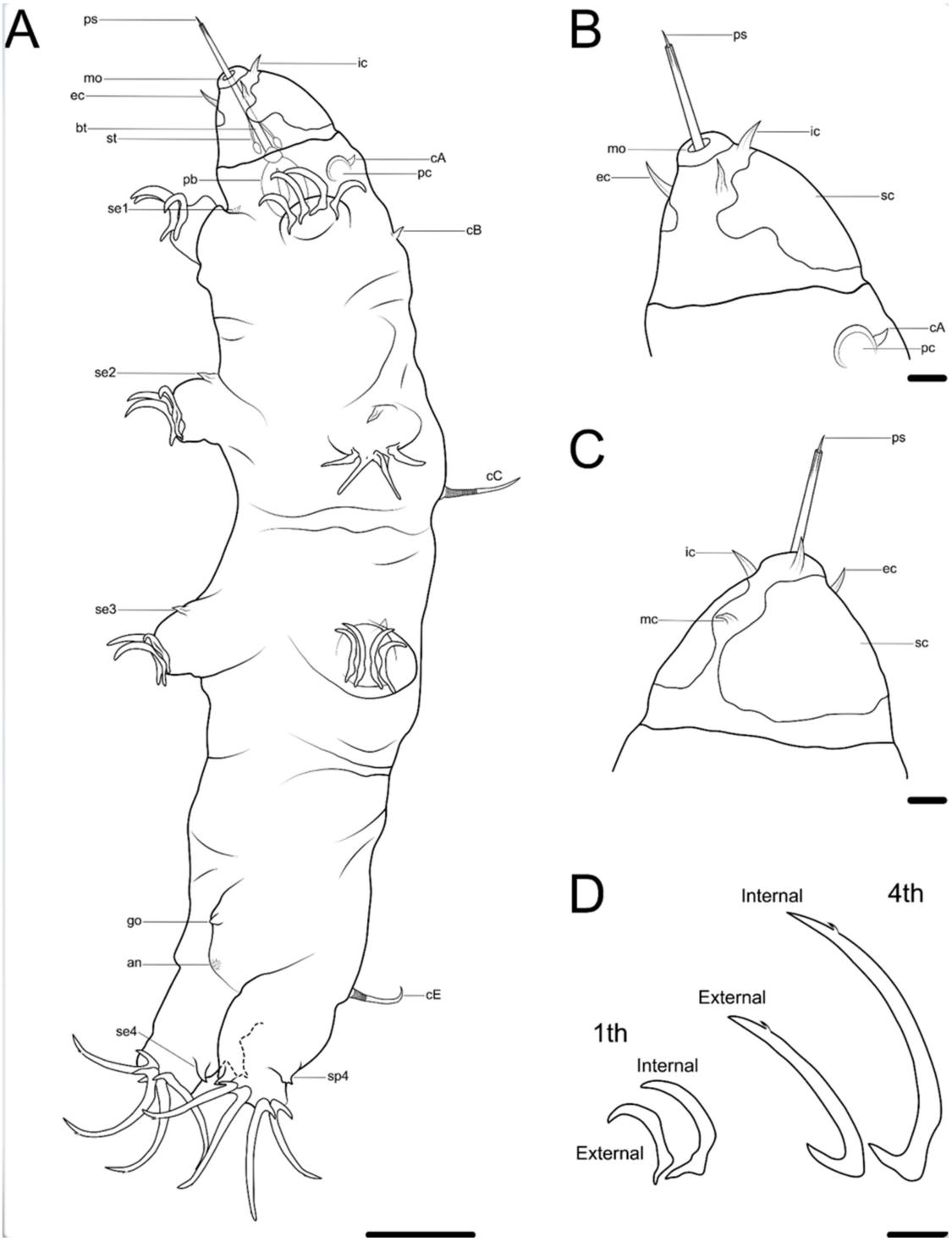

Figure 2. Drawing of *Coronarctus sonne* sp. nov. based on the holotype. (**A**) Habitus, ventral view; (**B**) Ventral view of the head; (**C**) Dorsal view of the head; (**D**) Claws on legs I and IV. The letter designations are as follows: an—anus; bt—buccal tube; cA—lateral cirrus *A*; cB—cirrus *B*; cC—cirrus *C*; cE—cirrus *E*; ec—external cirrus; go—gonopore; ic—internal cirrus; mc—median cirrus; mo—mouth opening; pb—pharyngeal bulb; pc—primary clava; ps—piercing stylet; sc—secondary clava; se1–4—sensory organ legs I–IV; sp4—coxal process on legs IV; st—stylet. Scale bars: (**A**)—50 μm; (**B**–**D**)—10 μm.

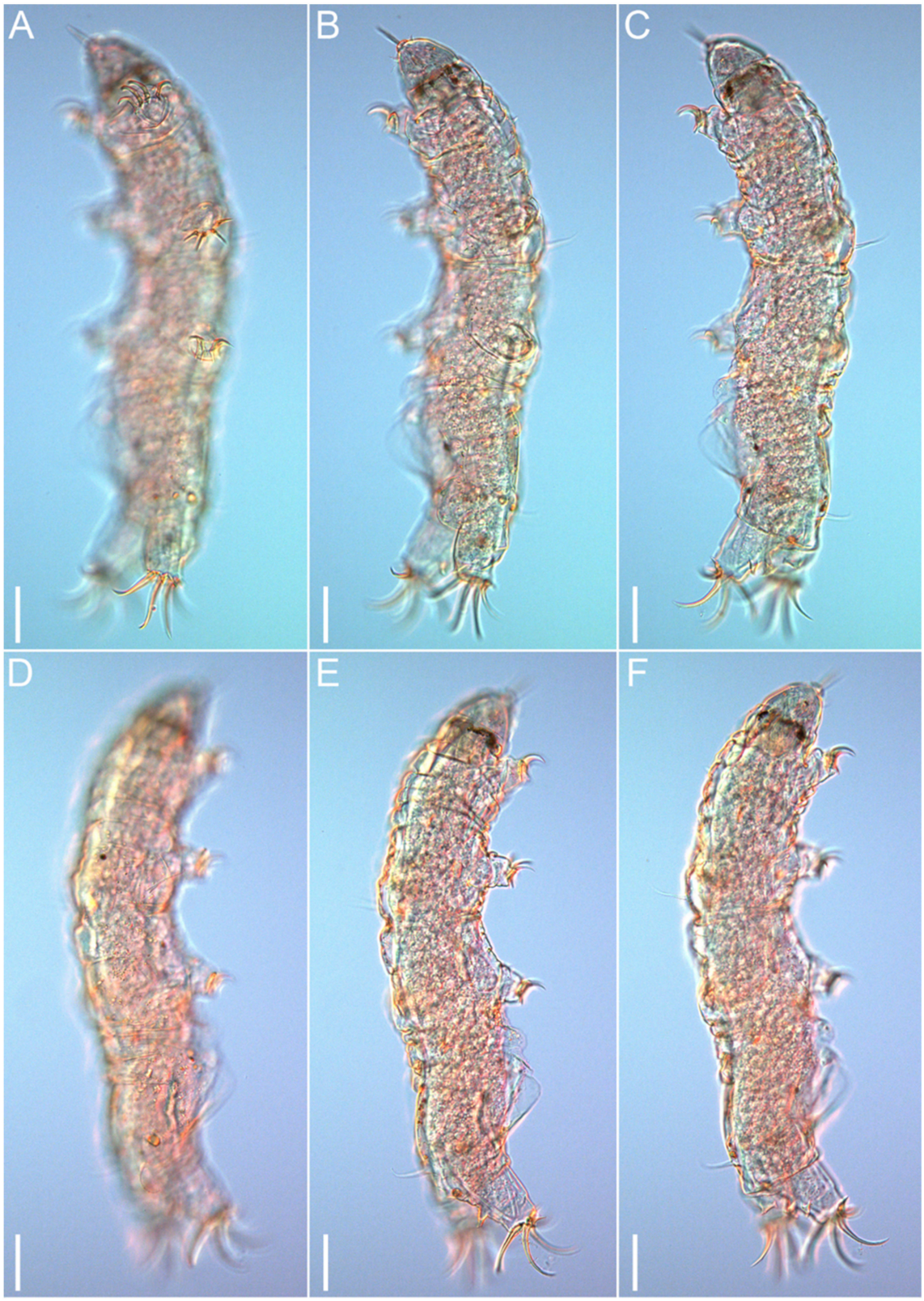

Figure 3. *Coronarctus sonne* sp. nov. Male holotype. (**A**–**C**) Habitus, ventrolateral view. (**D**–**F**) Habitus, dorsolateral view. Scale bars: 50 µm.

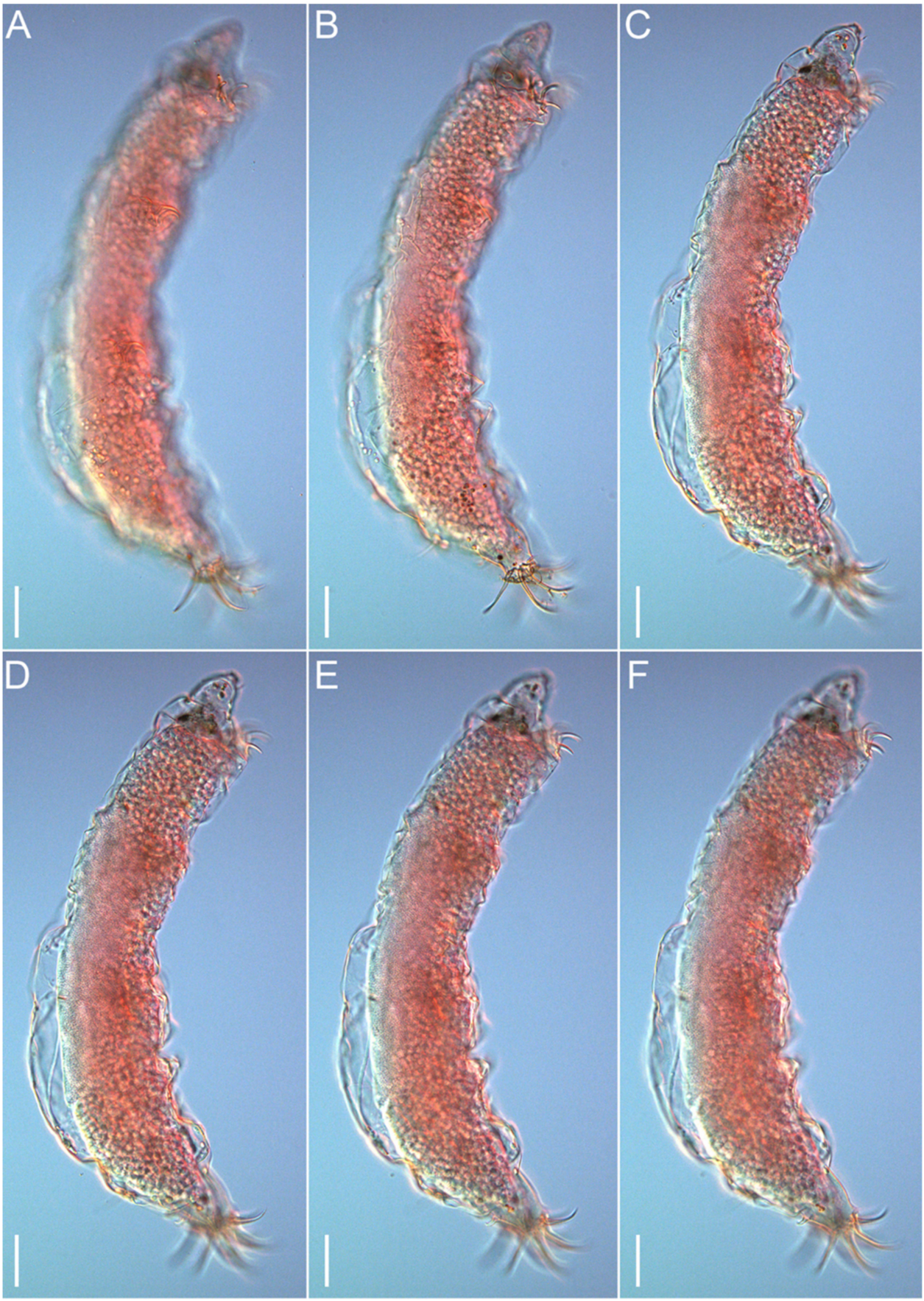

Figure 4. *Coronarctus sonne* sp. nov. (**A**–**F**) Female paratype, lateral view. Scale bars: 50 µm.

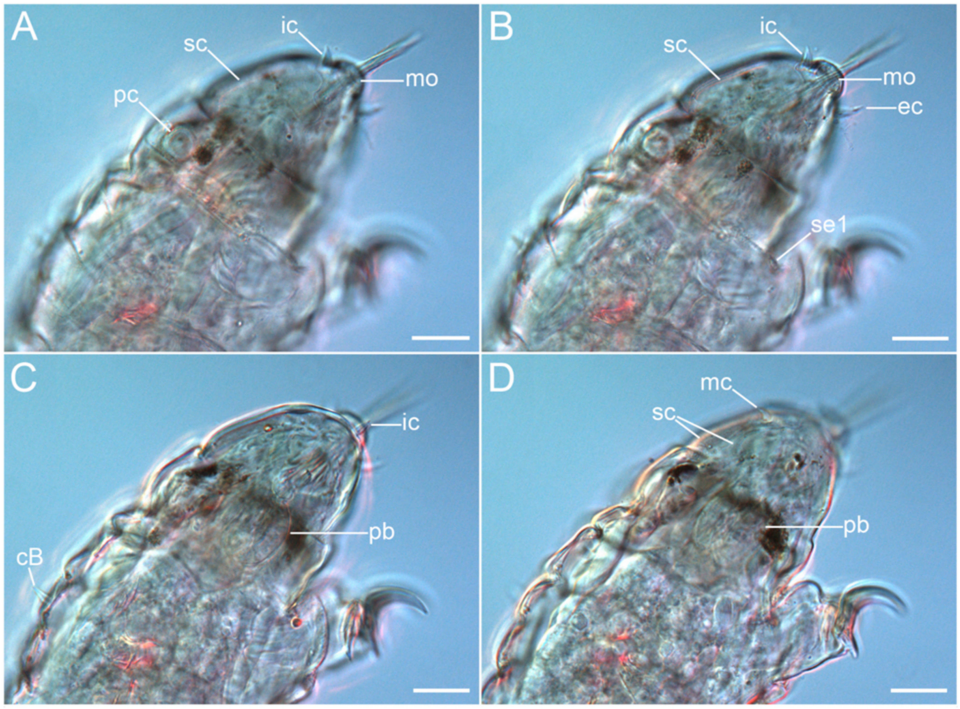

Figure 5. *Coronarctus sonne* sp. nov. Male holotype. (**A**,**B**) Ventrolateral view of the cephalic region; (**C**,**D**) Dorsolateral view of the cephalic region. The letter designations are as follows: cB—cirrus *B*; ec—external cirrus; ic—internal cirrus; mc—median cirrus; mo—mouth opening; pb—pharyngeal bulb; pc—primary clava; sc—secondary clava; se1—sensory organ legs I. Scale bars: 20 µm.

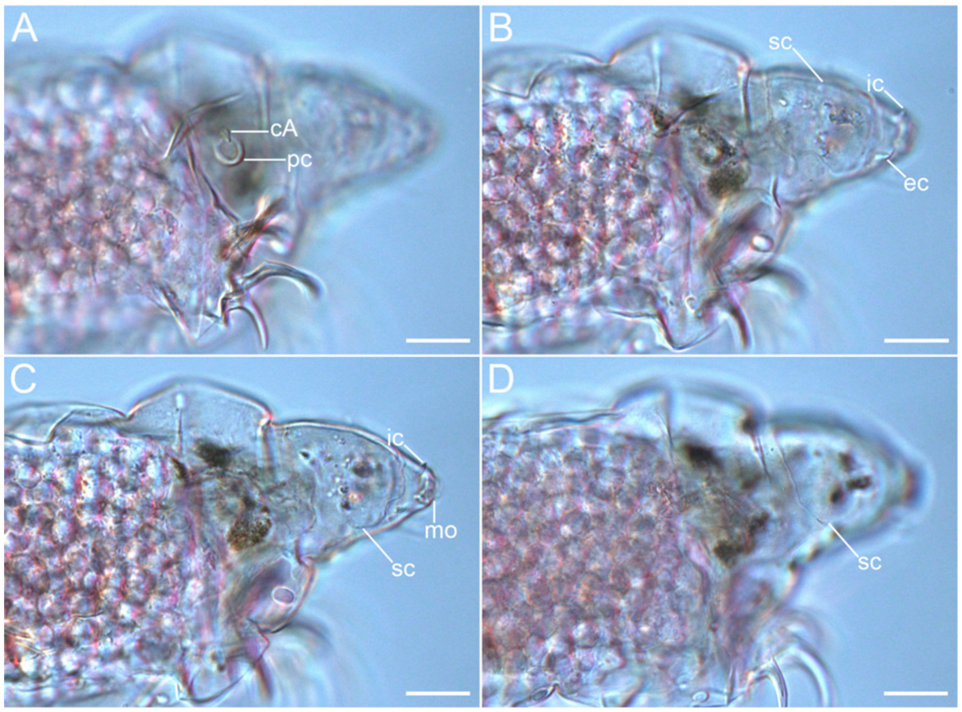

Figure 6. *Coronarctus sonne* sp. nov. (**A**–**D**) Lateral view of the cephalic region, female paratype. The letter designations are as follows: cA—lateral cirrus *A*; ec—external cirrus; ic—internal cirrus; mo—mouth opening; pc—primary clava; sc—secondary clava. Scale bars: 20 µm.

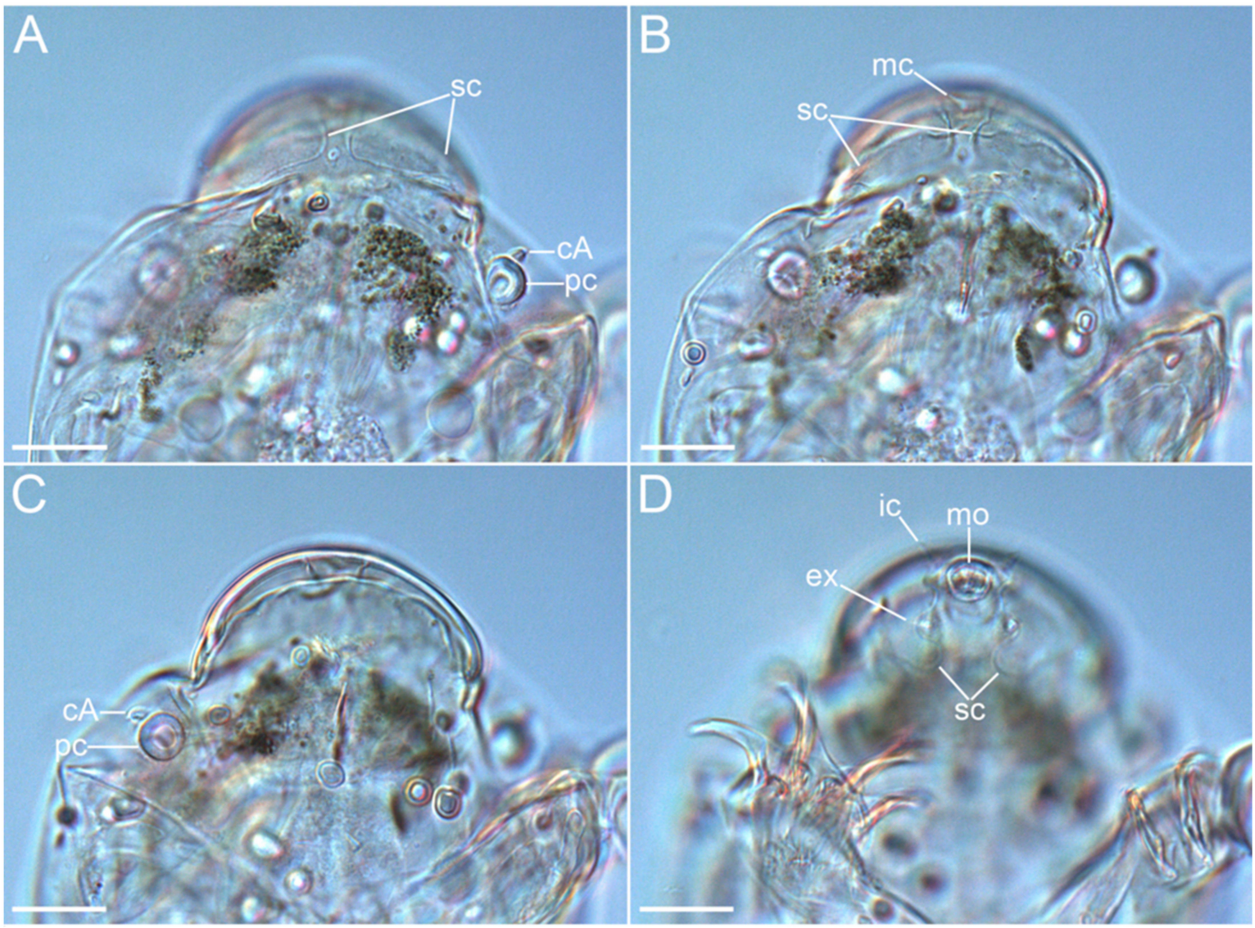

Figure 7. *Coronarctus sonne* sp. nov. Male paratype. (**A**,**B**) Ventral view of the cephalic region; (**C**,**D**) Dorsal view of the cephalic region. The letter designations are as follows: cA—lateral cirrus *A*; ec—external cirrus; ic—internal cirrus; mc—median cirrus; mo—mouth opening; pc—primary clava; sc—secondary clava. Scale bars: 20 μm.

3.1.1. Diagnosis

A *Coronarctus* with reduced leaf-shaped cephalic appendages and strongly pronounced heteromorphy of the claws. The median cirrus is inserted between the anterior and posterior dorsal lobes of the secondary clavae. The primary clavae are spherical in shape. Flattened secondary clavae with two dorsal and two ventral lobes that are not closely jointed. The cuticle is smooth. Sensory organs are present on each pair of legs. Legs IV have spine-like process inserted on the coxa. The claws of legs IV are much longer than the claws of the first three pairs of legs. All claws on legs IV have two points: an accessory point and a primary point.

3.1.2. Type Locality

An abyssal plain adjacent to the Kuril–Kamchatka Trench at depths of 5410 m (43°58.15′ N, 157°19.87′ E).

Additional Locality: 43°35.00′ N, 153°58.03′ E, 5378 m depth (Kuril–Kamchatka Trench).

3.1.3. Type Material

The male holotype, one female paratype, and one male paratype, collected at station KBI–1 (No. MIMB43528).

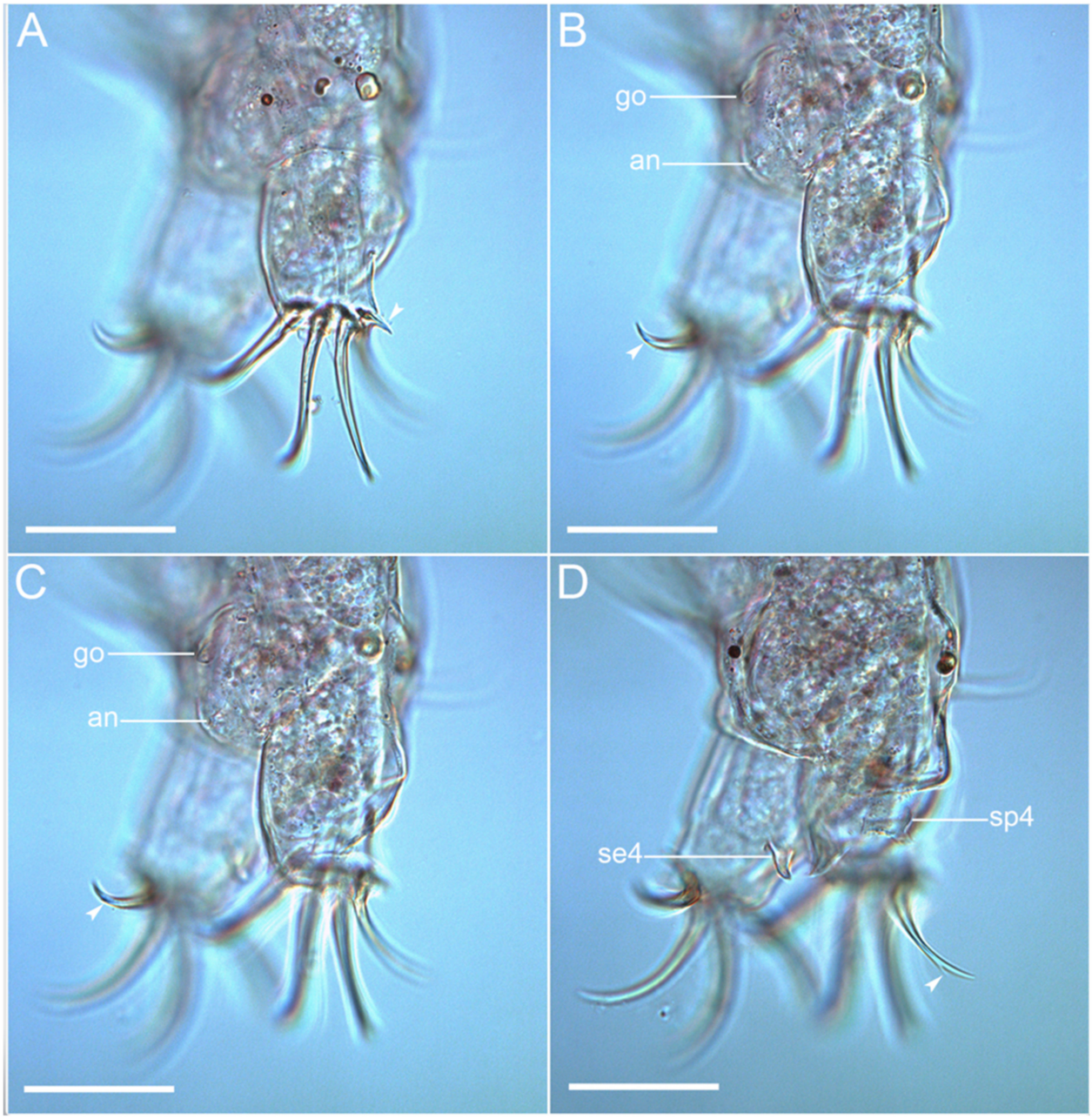

Figure 8. *Coronarctus sonne* sp. nov. (**A**–**D**) Caudal region of male holotype with the sensory organs on legs IV, male gonopore, and apical accessory spines on claws IV. The letter designations are as follows: an—anus; go—gonopore; se4—sensory organ legs IV; sp4—coxal process on legs IV. Arrows indicate two points: an accessory point and a primary point on claws IV. Scale bars: 50 µm.

3.1.4. Type Repository

All specimens were deposited in the Museum of the A.V. Zhirmunsky National Scientific Center of Marine Biology FEB RAS (Vladivostok, Russia).

3.1.5. Etymology

The species epithet *sonne* refers to the German RV *Sonne* on which the samples with the studied species were collected.

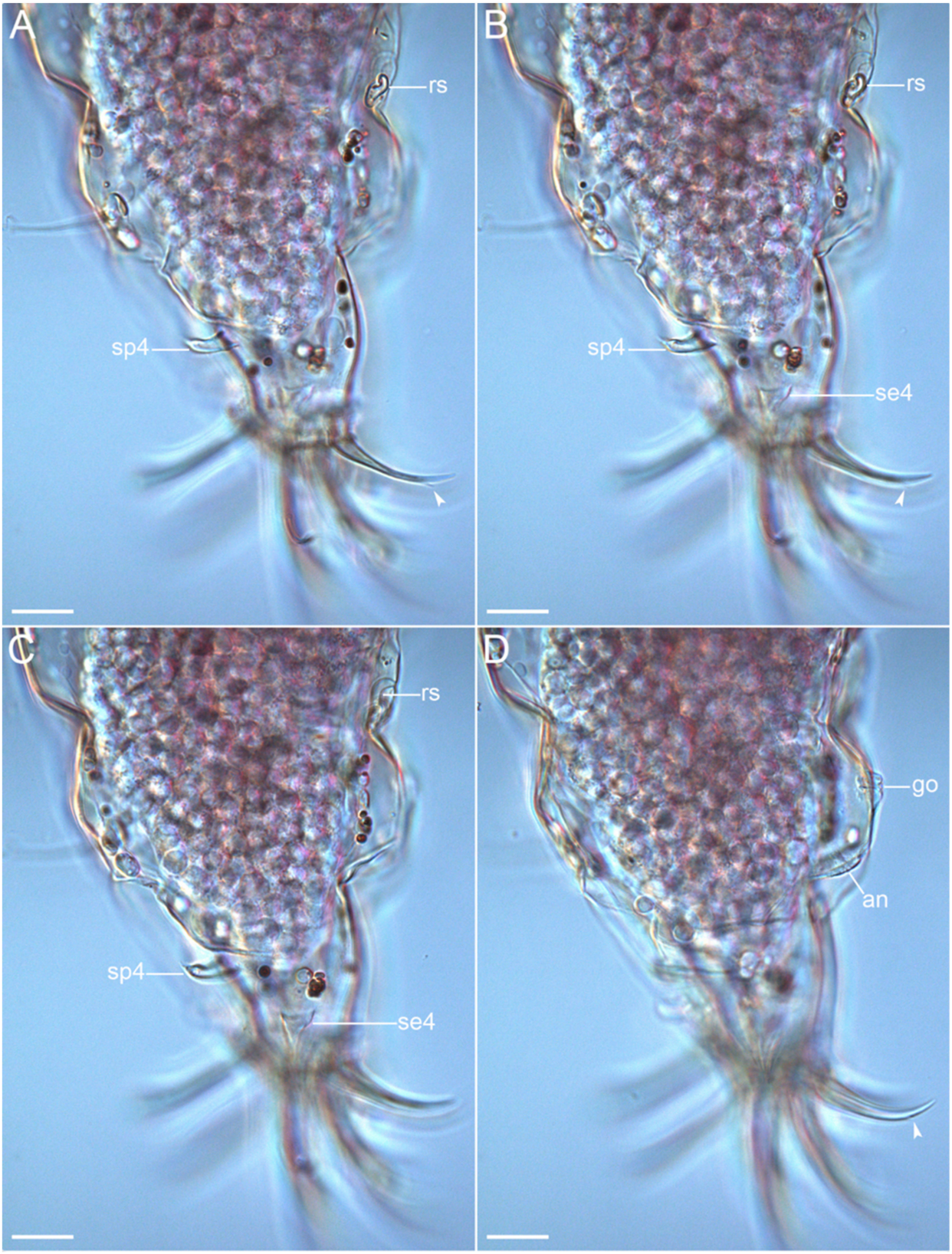

Figure 9. *Coronarctus sonne* sp. nov. (**A**–**D**) Female paratype. Lateral view of the caudal region with the sensory organs on legs IV, the female reproductive system, and the apical accessory spines on claws IV. The letter designations are as follows: an—anus; go—gonopore; se4—sensory organ legs IV; sp4—coxal process on legs IV; rs—seminal receptacle. Arrows indicate two points: an accessory point and a primary point on claws IV. Scale bars: 20 µm.

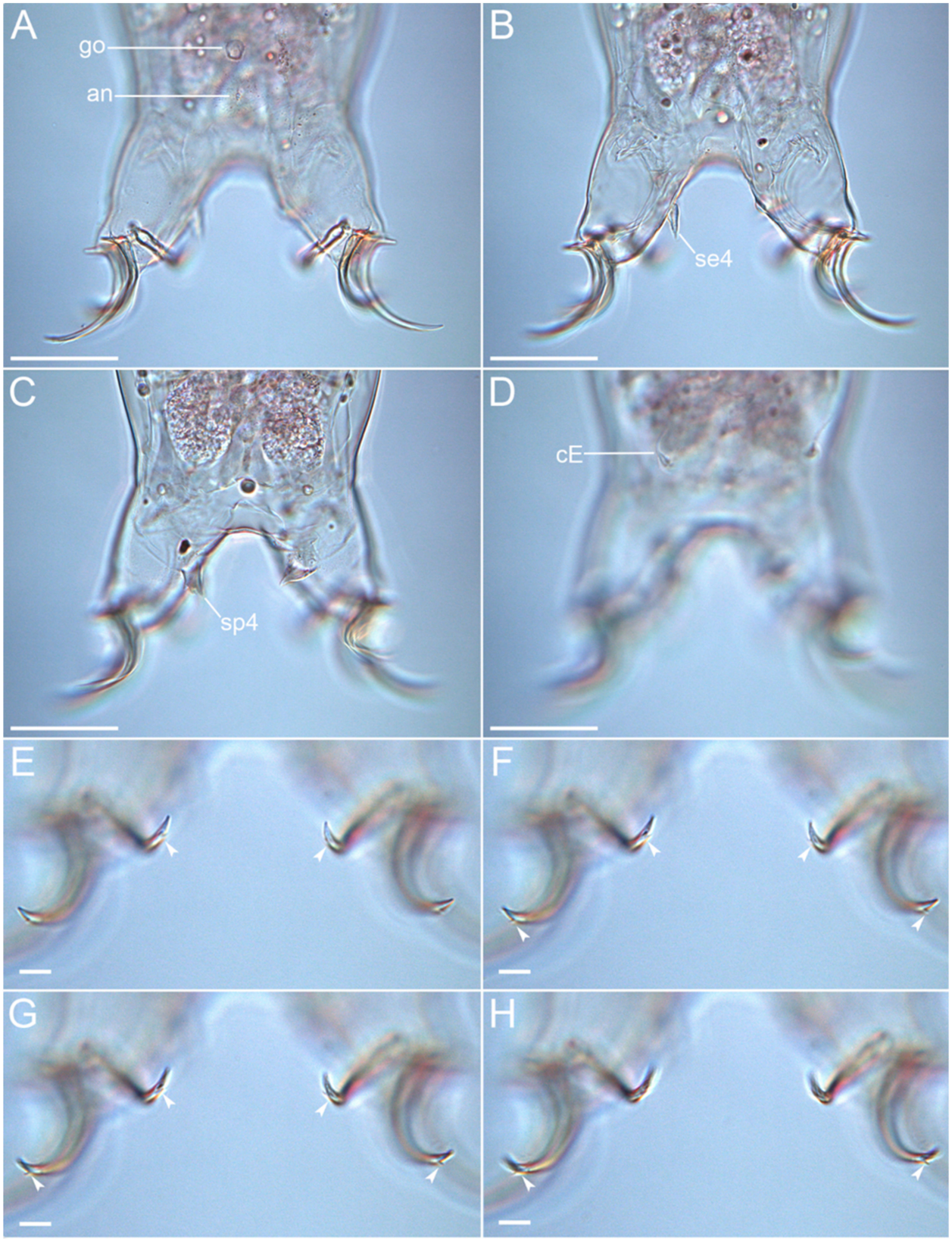

Figure 10. *Coronarctus sonne* sp. nov. Male paratype. (**A**,**B**) Ventral view of the caudal region; (**C**,**D**) Dorsal view of the caudal region; (**E**–**H**) External and internal claws on legs IV showing two points: an accessory point and a primary point (arrows). The letter designations are as follows: an—anus; go—gonopore; cE—cirrus *E*; se4—sensory organ legs IV; sp4—coxal process on legs IV. Scale bars: (**A**–**D**)—20 µm; (**E**–**H**)—10 µm.

3.1.6. Description of the Holotype

The holotype is an adult male with a long cylindrical body ca. 494 µm long and 104 µm wide (Figures 2A and 3). The cuticle is smooth and transparent. The head is narrower than the entire body and separated into two parts: an anterior triangular part with the leaf-shaped paired internal (9.6 µm long) and external cirri (10.1 µm long) and the unpaired median cirrus (5.3 µm long) and a posterior part with lateral cirri *A* (8.6 µm long) and primary clavae (8.7 µm in diameter). Paired internal and external cirri are located around the mouth opening; an unpaired short median cirrus is inserted between the anterior and posterior dorsal lobes of the secondary clavae (Figures 2B,C, 5 and 7B,D). The primary clavae are spherical in shape and are inserted separately from short leaf-shaped lateral cirrus *A* (Figures 2B, 5A, 6A and 7A,C). The secondary clavae are flattened, with two dorsal lobes and two ventral lobes each (Figures 2B and 7D). Tertiary clavae are absent.

Trunk cirri *B* (7.0 µm long), *C* (38.0 µm long), and *E* (36.3 µm long) present as a typical trait of the genus. Cirri *C* and *E* with short cirrophore, accordion-like scapus, and flagellum. Each of the legs are short and stocky. Short spine-like sensory organs are present on all pairs of legs (Figure 2A), almost similar in length on legs I–III (5.2, 8.4, and 9.0 µm long, respectively) and much longer on legs IV (19.0 µm long). Legs IV also have a spine-like process (15.2 µm long) inserted on the coxa (Figures 8D, 9A–C and 10C).

Claws display visible heteromorphy: claws on legs IV (external and internal claws are 48.3/45.1 and 55.7/56.5 µm long, respectively) are much longer than claws on legs I (external and internal claws are 26.2/26.4 and 36.8/32.1 µm long, respectively). On all legs, internal claws are slightly longer than external claws (Table 2). All claws of the fourth pair of legs are slightly curved and have long sharp basal spurs and two apical accessory spines (Figures 2D and 10E–H).

The mouth opening is terminal and surrounded by radial cuticular folds. The pharyngeal bulb is oval-shaped (26.3 µm long and 16.9 µm wide); placoids were not observed (Figure 5C,D). Stylet is present, protruding out of the mouth opening (51.0 µm long). The male gonopore, in form of a triangular slit, is located 16.8 µm from anus (Figures 8B,C and 10A). The anal fissure is surrounded by a wrinkled cuticle. In the female paratype, the seminal receptacle has an unclear shape and is located next to a rosette-like gonopore. The distance between the gonopore and anus is 22.5 µm.

3.1.7. Differential Diagnosis

The currently known *Coronarctus* species are divided into two main groups, depending on the sizes of the cephalic appendages and the ratio of the sizes of the claws on legs I–III and claws IV [13]. Species of the *Cor. tenellus* group exhibit claw heteromorphy (claws on legs IV are much longer than the claws of legs I–III) and have short cephalic appendages. Species of the *Cor. stylisetus* group display claw homomorphy (claws on all legs are similar in length) and long cephalic appendages. The strongly pronounced heteromorphy of the claws and the sizes of the cephalic appendages allow attributing the new species, *Coronarctus sonne* sp. nov., to the *Cor. tenellus* group. The seven previously described species of the genus *Coronarctus* also show claw heteromorphy and have short cephalic appendages: *Cor. tenellus* Renaud-Mornant, 1987; *Cor. disparilis* Renaud-Mornant, 1987; *Cor. laubieri* Renaud-Mornant, 1987; *Cor. mexicus* Romano III, Gallo, D'Addabbo, Accogli, Baguley, and Montagna, 2011; *Cor. dissimilis* Gomes-Júnior, Santos, da Rocha, Santos, and Fontoura, 2019; *Cor. neptunus* Gomes-Júnior, Santos, da Rocha, Santos, and Fontoura, 2019; and *Cor. yurupari* Gomes-Júnior, Santos, da Rocha, Santos, and Fontoura, 2019 [13,21,22].

The new species can be distinguished from all those species by having two points, an accessory point and a primary point, on both the internal and external claws on legs IV. Moreover, it differs from:

Cor. laubieri and *Cor. dissimilis* by the median cirrus located after the posterior dorsal lobes and near the posterior edges of the secondary clavae and the deep recesses in the secondary clavae on the ventral side of the body.

Cor. mexicus by the presence of three ventral lobes of the secondary clavae and short cephalic cirri with a long accordion-like scapus instead of leaf-like cephalic cirri.

Cor. yurupari by the pedunculated primary clavae and the presence of the apical accessory spines on all claws of legs I–III.

Cor. neptunus by a leg I-III sensory organ consisting of a needle-like structure protruding from the wrinkled broad cylindrical basal portion. Moreover, lateral cirri *A* in *Cor. neptunus* consist of an annulated scapus followed by a smooth flagellum ending in a spherical tip.

Cor. tenellus by the lack of coxal spine-like processes on legs IV.

Cor. disparilis by the closely articulated ventral lobes of the secondary clavae and the presence of the additional spine on the inner side of the claws on legs IV.

3.2. Taxonomy

Family Halechiniscidae Thulin, 1928
Subfamily Euclavarctinae Renaud-Mornant, 1983
Genus *Moebjergarctus* Bussau, 1992
Moebjergarctus okhotensis sp. nov.
(Figures 11–21, Table 3)
urn:lsid:zoobank.org:act:A343583C-1E0B-4156-922E-D576CAAB65A2

Table 3. Body measurements (in μm) of *Moebjergarctus okhotensis* sp. nov. type series. Body width was measured between legs III and IV; ?—trait not measurable. The values in the table for paratypes are presented as minimum and maximum values ± standard deviations.

Character	Holotype, Female	Paratypes	
		Males (n = 6)	Females (n = 4)
Body length	230.7	188.4–276.7 ± 35.5 (n = 6)	195.9–246.7 ± 21.1 (n = 4)
Body width	92.4	75.8–95.6 ± 9.0 (n = 5)	74.5–79.9 ± 3.8 (n = 2)
Head width	48.3	34.9–44.1 ± 3.5 (n = 5)	?
Median cirrus	8.2	?	6.3–9.9 ± 1.6 (n = 4)
Internal cirrus	7.4	5.6–8.5 ± 1.1 (n = 5)	5.6–7.4 ± 0.9 (n = 3)
External cirrus	11.3	8.7–12.2 ± 1.4 (n = 6)	8.8–11.5 ± 1.4 (n = 3)
Cirrus *A*	14.3	12.1–14.0 ± 0.8 (n = 5)	11.6–13.9 ± 1.7 (n = 2)
Primary clava	12.0	11.3–13.9 ± 1.0 (n = 6)	10.9–12.6 ± 0.8 (n = 4)
Secondary clava	4.8	3.4–4.5 ± 0.5 (n = 6)	4.0–4.6 ± 0.2 (n = 4)
Cirrus *E*	?	30.4–66.0 ± 15.5 (n = 6)	29.2–41.8 ± 6.7 (n = 3)
Sensory organ on leg I	5.8	5.1–6.8 ± 0.8 (n = 5)	5.6–5.8 ± 0.1 (n = 2)
Sensory organ on leg II	6.0	4.8–6.6 ± 0.8 (n = 4)	4.5–6.1 ± 1.1 (n = 2)
Sensory organ on leg III	5.1	4.6–5.2 ± 0.3 (n = 3)	?
Sensory organ on leg IV	4.8	4.2–4.9 ± 0.3 (n = 6)	3.6–5.1 ± 0.8 (n = 3)
Internal digits on legs I–III	8.9	9.7–12.7 ± 1.3 (n = 6)	10.2–12.0 ± 0.9 (n = 4)
External digits on legs I–III	7.1	7.0–9.5 ± 0.9 (n = 6)	7.3–9.4 ± 0.9 (n = 4)
Internal digits legs IV	12.7	11.3–19.1 ± 2.8 (n = 6)	14.2–15.9 ± 0.9 (n = 3)
External digits legs IV	10.3	8.1–14.4 ± 2.3 (n = 6)	9.9–12.2 ± 1.2 (n = 3)
Caudodorsal bulge	5.4	2.9–7.8 ± 1.9 (n = 6)	2.5–9.1 ± 3.1 (n = 4)

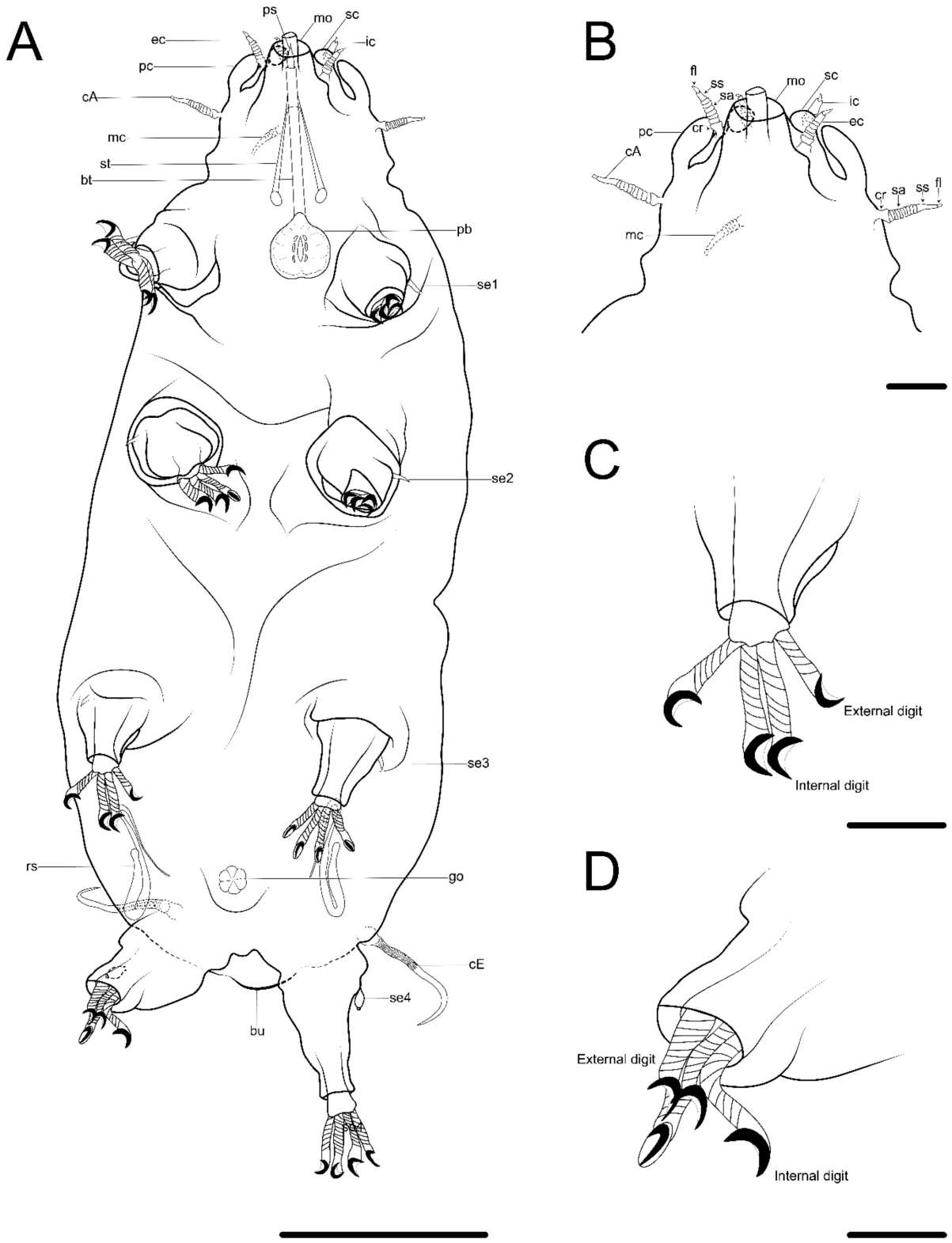

Figure 11. Drawing of *Moebjergarctus okhotensis* sp. nov. based on the holotype. (**A**) Habitus, ventral view; (**B**) Ventral view of the head; (**C**) Leg I with digits; (**D**) Leg IV with digits. The letter designations are as follows: bt—buccal tube; bu—caudodorsal bulge; cA—lateral cirrus *A*; cE—cirrus *E*; cr—cirrophore; ec—external cirrus; fl—flagellum; go—gonopore; ic—internal cirrus; mc—median cirrus; mo—mouth opening; pb—pharyngeal bulb; pc—primary clava; ps—piercing stylet; rs—seminal receptacle; sa—annulated portion of the scapus; sc—secondary clava; se1–4—sensory organ legs I–IV; ss—smooth portion of the scapus; st—stylet. Scale bars: (**A**)—50 μm; (**B**–**D**)—10 μm.

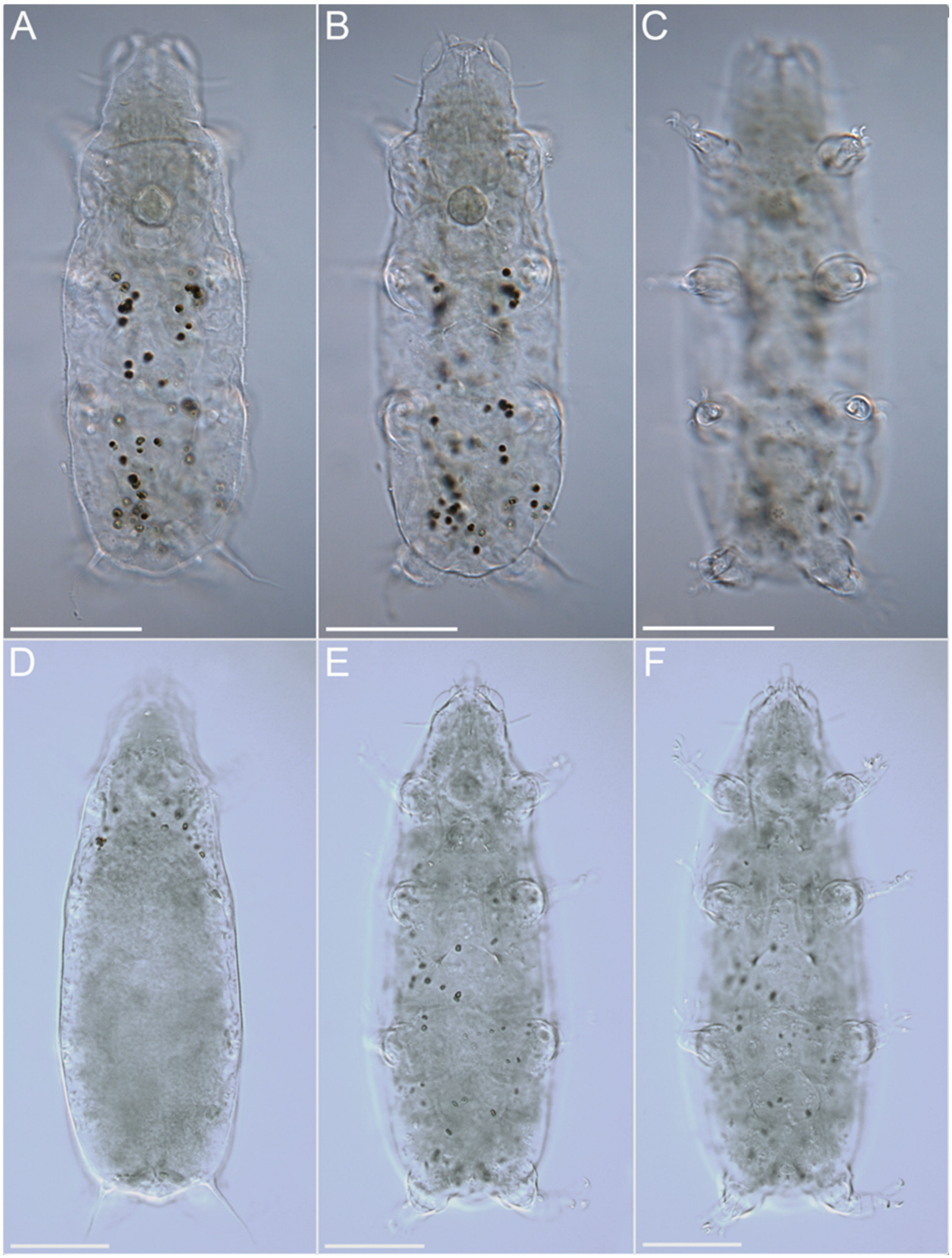

Figure 12. *Moebjergarctus okhotensis* sp. nov. (**A**–**C**) Habitus of female paratype; (**D**–**F**) Habitus of male paratype. Scale bars: 50 μm.

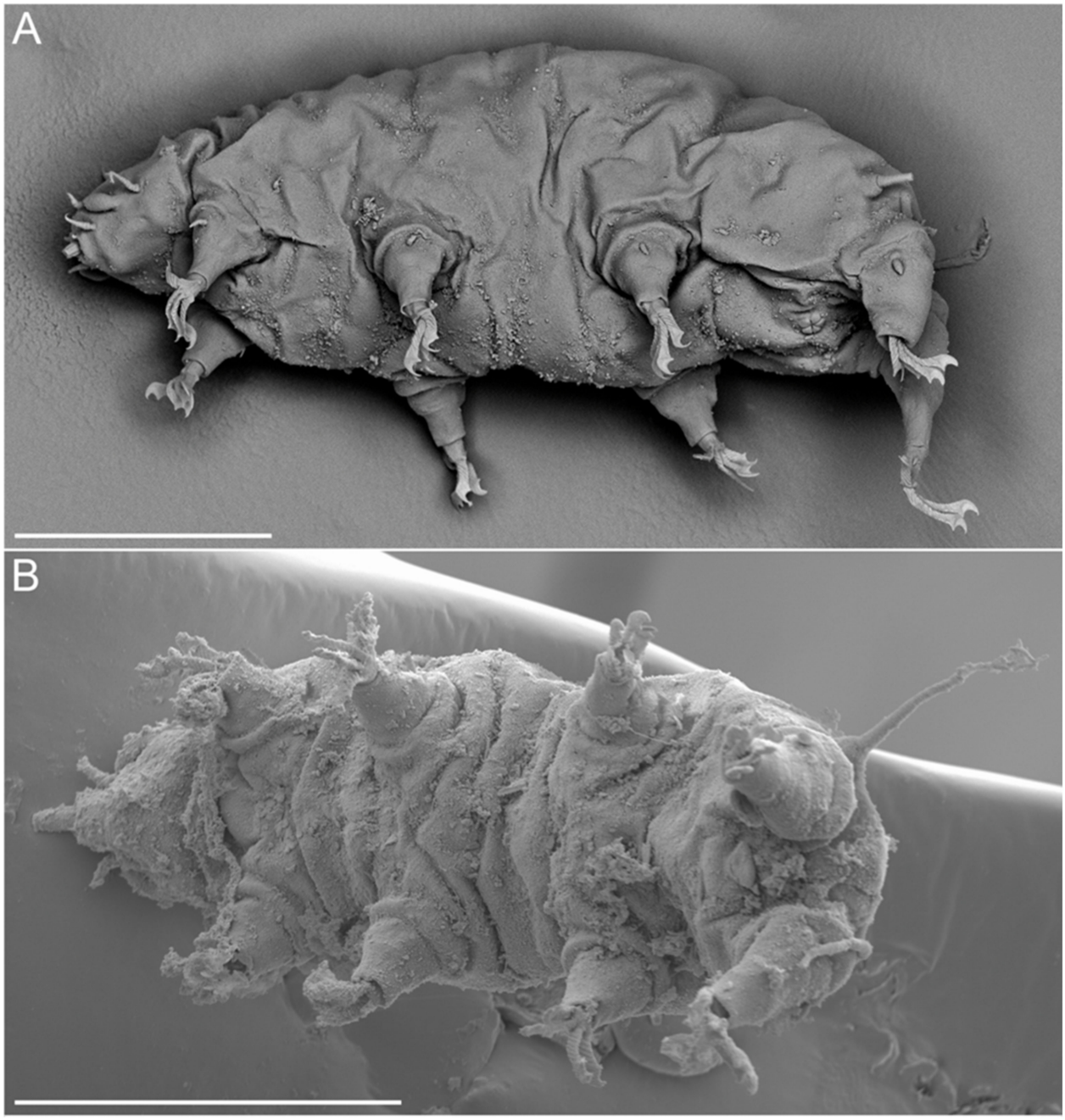

Figure 13. *Moebjergarctus okhotensis* sp. nov. Scanning electron microscopy. (**A**) Female habitus; (**B**) Male habitus. Scale bars: 50 μm.

3.2.1. Diagnosis

A *Moebjergarctus* with an ovate-shaped body. A conical head bears eleven cephalic sensory organs (unpaired median cirrus, paired internal cirri, paired external cirri, paired cirri *A*, paired primary clavae, and paired secondary clavae). All cephalic cirri are divided into three parts: a cirrophore, a long scapus with annulated and smooth parts, and a short flagellum. The primary clavae are club-shaped. The secondary clavae are spherical in shape. The sensory organs on legs I are split. The sensory organs on legs II–III are spine-shaped. The small papilla on legs IV have short tips. Cirri *E* are long. Corkscrew-shaped digits have simple crescent-shaped claws. The digits on legs I–III are shorter than on legs IV, with external digits that are also shorter than the internal digits. The caudodorsal bulge is present, covered by a crescent-shaped cuticular thickening.

3.2.2. Type Locality

The Kuril Basin (the Sea of Okhotsk): 47°12.0′ N, 149°37.0′ E, 3366 m depth (station SB6).

Additional Locality: the Kuril Basin (the Sea of Okhotsk), 48°03.0′ N, 150°00.3′ E, 3351 m depth.

3.2.3. Type Material

The female holotype, two female paratypes, and two males paratypes were collected at station SB6 (No. MIMB43529); four males, two females, and one paratype of unidentified sex were collected at station SB4 (No. MIMB43530).

Other material: seven specimens embedded in the same slide as the holotype (No. MIMB43529), with damaged and with poorly distinguishable morphological characteristics; five males; and two SEM specimens.

3.2.4. Type Repository

All specimens were deposited in the Museum of the A.V. Zhirmunsky National Scientific Center of Marine Biology FEB RAS (Vladivostok, Russia).

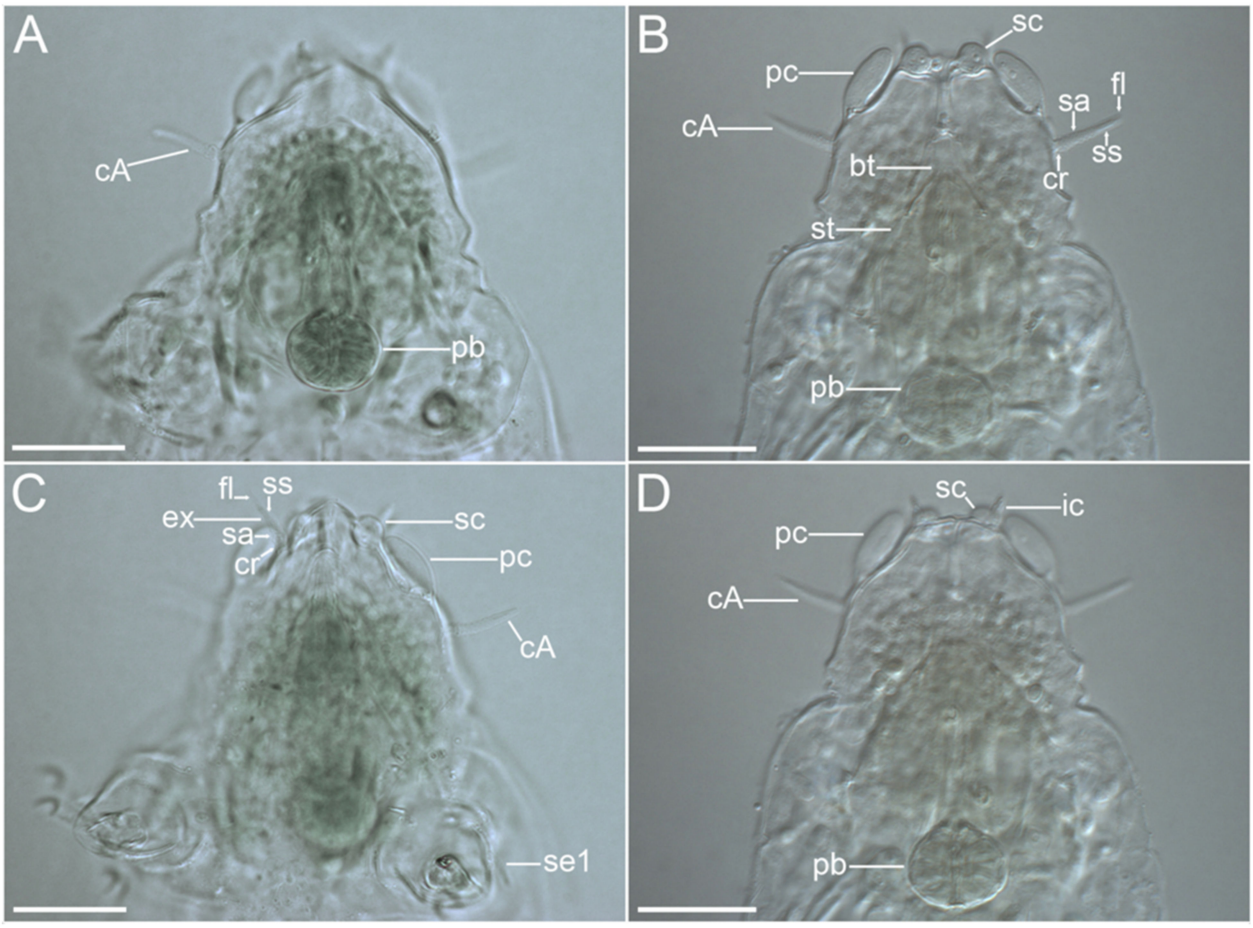

Figure 14. *Moebjergarctus okhotensis* sp. nov. Cephalic region with the sensory organs and the structure of the cephalic cirri. (**A**,**C**) Female holotype; (**B**,**D**) Male paratype. The letter designations are as follows: bt—buccal tube; cA—lateral cirrus *A*; cr—cirrophore; ec—external cirrus; fl—flagellum; ic—internal cirrus; pb—pharyngeal bulb; pc—primary clava; sa—annulated portion of the scapus; sc—secondary clava; se1—sensory organ legs I; ss—smooth portion of the scapus; st—stylet. Scale bars: 20 μm.

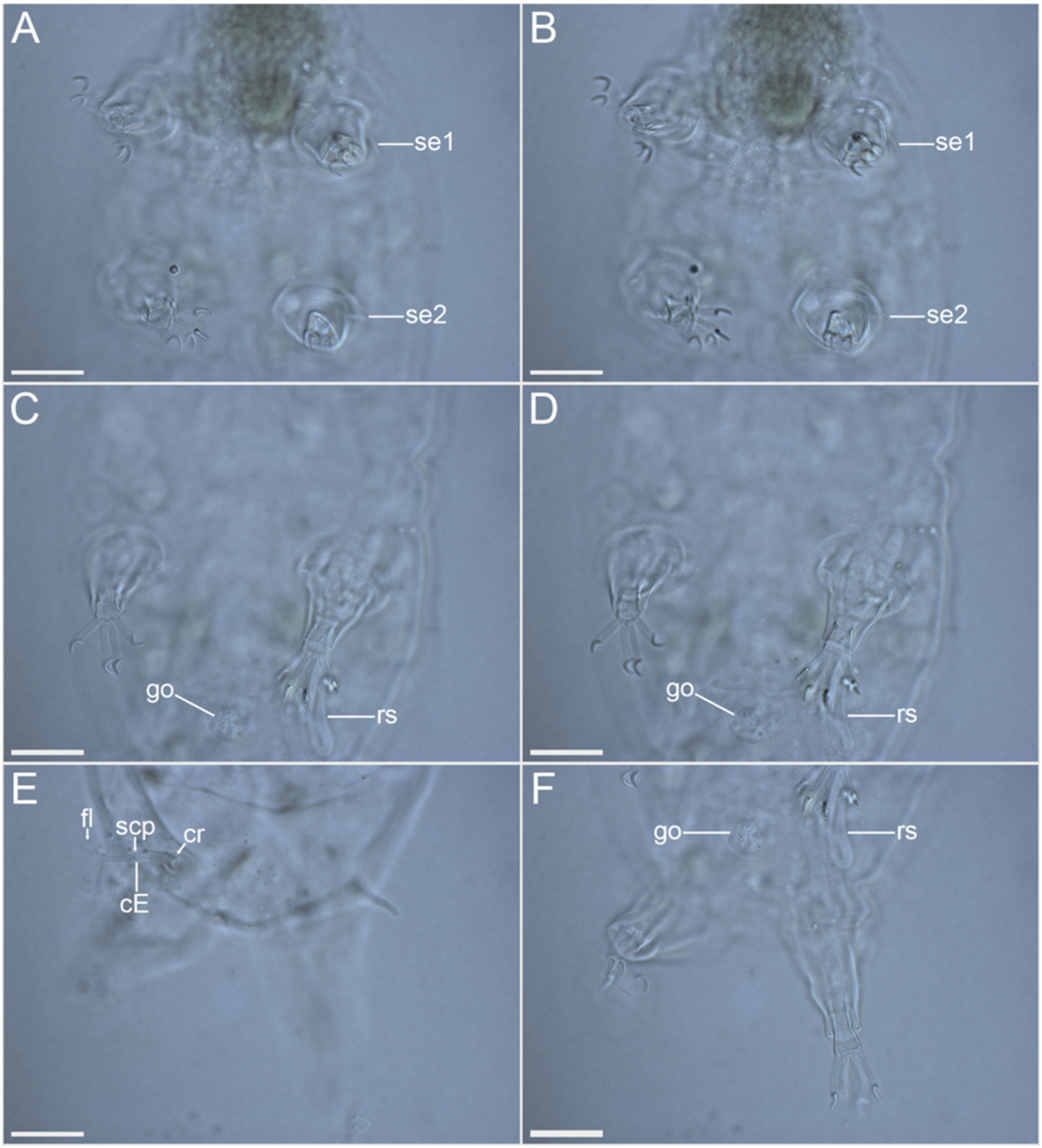

Figure 15. *Moebjergarctus okhotensis* sp. nov. Female holotype. (**A**,**B**) Legs I and II with digits and sensory organs, ventral view; (**C**,**D**) Legs III with digits and female reproductive system, ventral view; (**E**) Caudal region with cirrus *E*, dorsal view; (**F**) Legs IV with digits and female reproductive system, ventral view. The letter designations are as follows: cE—cirrus *E*; cr—cirrophore; fl—flagellum; go—gonopore; rs—seminal receptacle; scp—scapus; se1–4—sensory organ legs I–IV. Scale bars: 20 µm.

3.2.5. Etymology

The species epithet *okhotensis* refers to the Sea of Okhotsk.

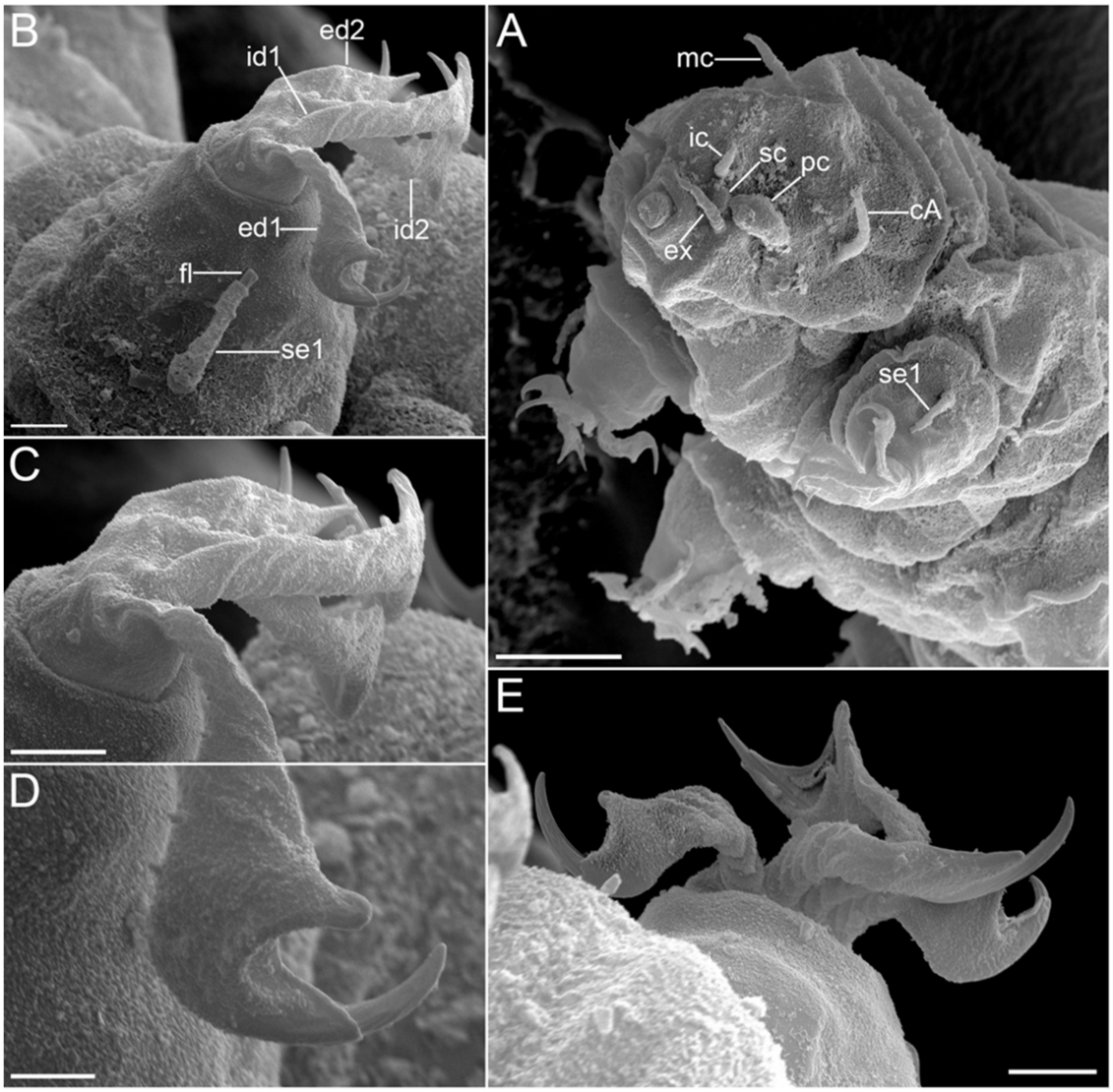

Figure 16. *Moebjergarctus okhotensis* sp. nov. Scanning electron microscopy. (**A**) Head with the cephalic sensory organs; (**B**) Leg I (left) with corkscrew-shaped digits and simple crescent-shaped claws; (**C**) Legs I corkscrew-shaped digits; (**D**) Simple crescent-shaped claw; (**E**) Leg I (right) with corkscrew-shaped digits and simple crescent-shaped claws. The letter designations are as follows: cA—lateral cirrus *A*; ec—external cirrus; ed1 and ed2—external digits; ec—external cirrus; fl—flagellum; ic—internal cirrus; id1 and id2—internal digits; mc—median cirrus; pc—primary clava; sc—secondary clava; se1—sensory organ legs I. Scale bars: (**A**)—10 µm; (**B**,**C**,**E**)—2 µm; (**D**)—1 µm.

3.2.6. Description of the Holotype

The holotype is an adult female. The body is ovate-shaped, ca. 230.7 µm long, and 92.4 µm wide (Figure 11A). The head is conical and 48.3 µm wide, bearing eleven cephalic sensory organs (Figures 11B, 14 and 17A). The primary clavae are club-shaped (12.0 µm long) and bent forward; the secondary clavae are spherical in shape (4.8 µm in diameter); and the tertiary clavae are not visible. Each cephalic cirrus contains three parts: a short cirrophore, a long scapus with an annulated proximal portion and a smooth distal portion ending in a blunt tip, and a very short flagellum (Figures 11B, 14B,C and 16A). The segments of the scapus were not always visible using light microscopy but were observed under SEM. The median cirrus is 8.2 µm long. The paired cirri *A* are 14.3 µm long and separated from the primary clavae. The paired external cirri are 11.3 µm long (1.8 µm cirrophore; 7.3 µm scapus; and 2.2 µm flagellum). The dorsal internal cirrus is 7.4 µm in length. The

paired cirri *E* are inserted on a short cirrophore dorsal to the coxae of legs IV, each with a cirrophore, annulated scapus, and flagellum (Figures 15E and 18C,D). In many individuals, including the holotype, cirri *E* were broken off, which made it difficult to measure their true lengths. The sensory organs on legs I (5.8 µm) are divided into a cirrophore, a scapus, and a short tubular tip (Figure 16B). The sensory organs on legs II–III are spine-shaped (Figure 17A,B) (6.0 µm on legs II and 5.1 µm on legs III). The sensory organs on legs IV are in the form of small 4.8 µm long papilla with short protruding tips (Figures 17E and 18A,B,E).

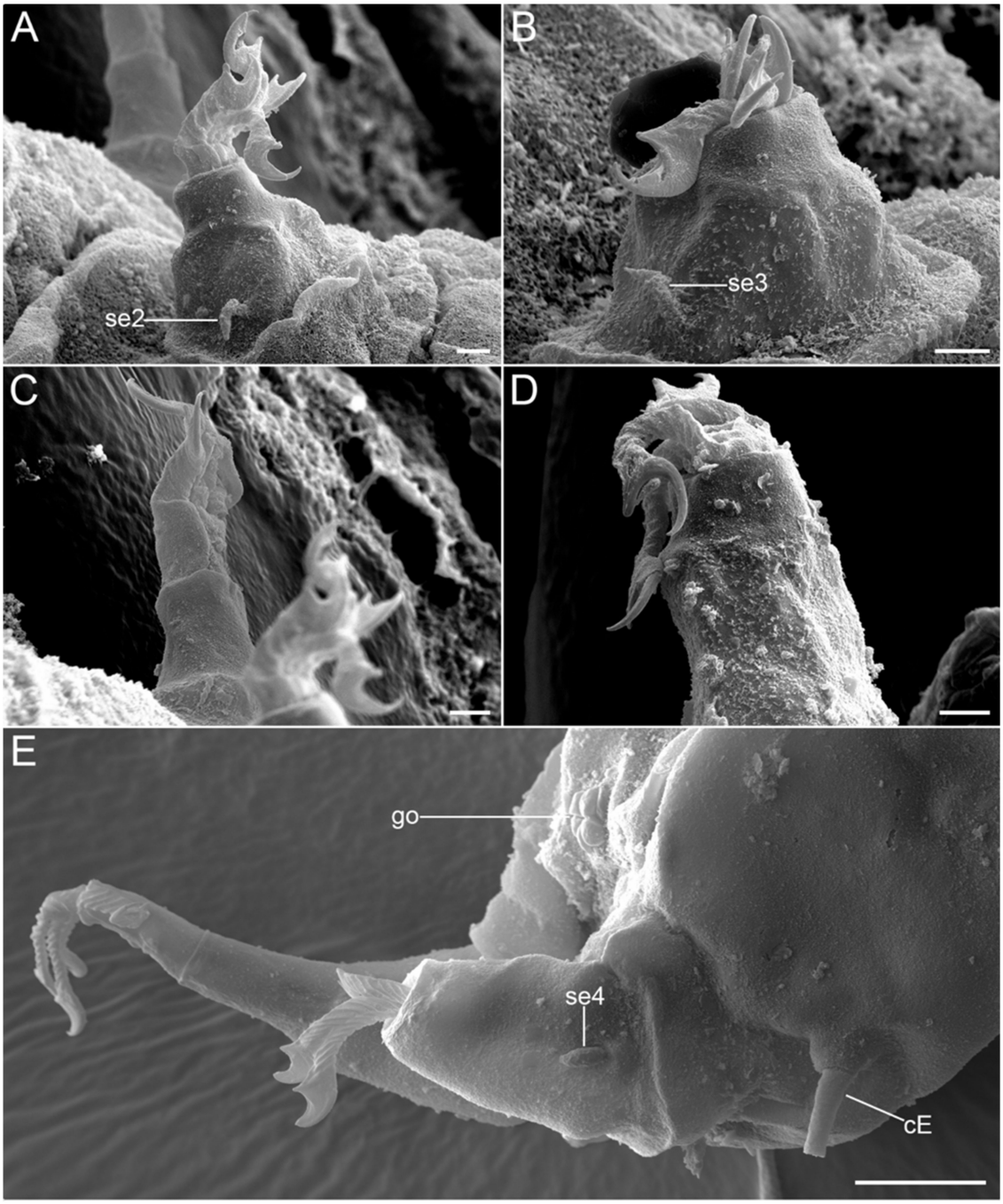

Figure 17. *Moebjergarctus okhotensis* sp. nov. Scanning electron microscopy. (**A**) Leg II (left); (**B**) Leg III (left); (**C**) Leg II (right); (**D**) Leg IV (left); (**E**) Caudal region with the sensory organs on leg IV and the female gonopore. The letter designations are as follows: cE—cirrus *E*; go—gonopore; se2–4—sensory organ legs II–IV. Scale bars: (**A**–**D**)—2 µm; (**E**)—10 µm.

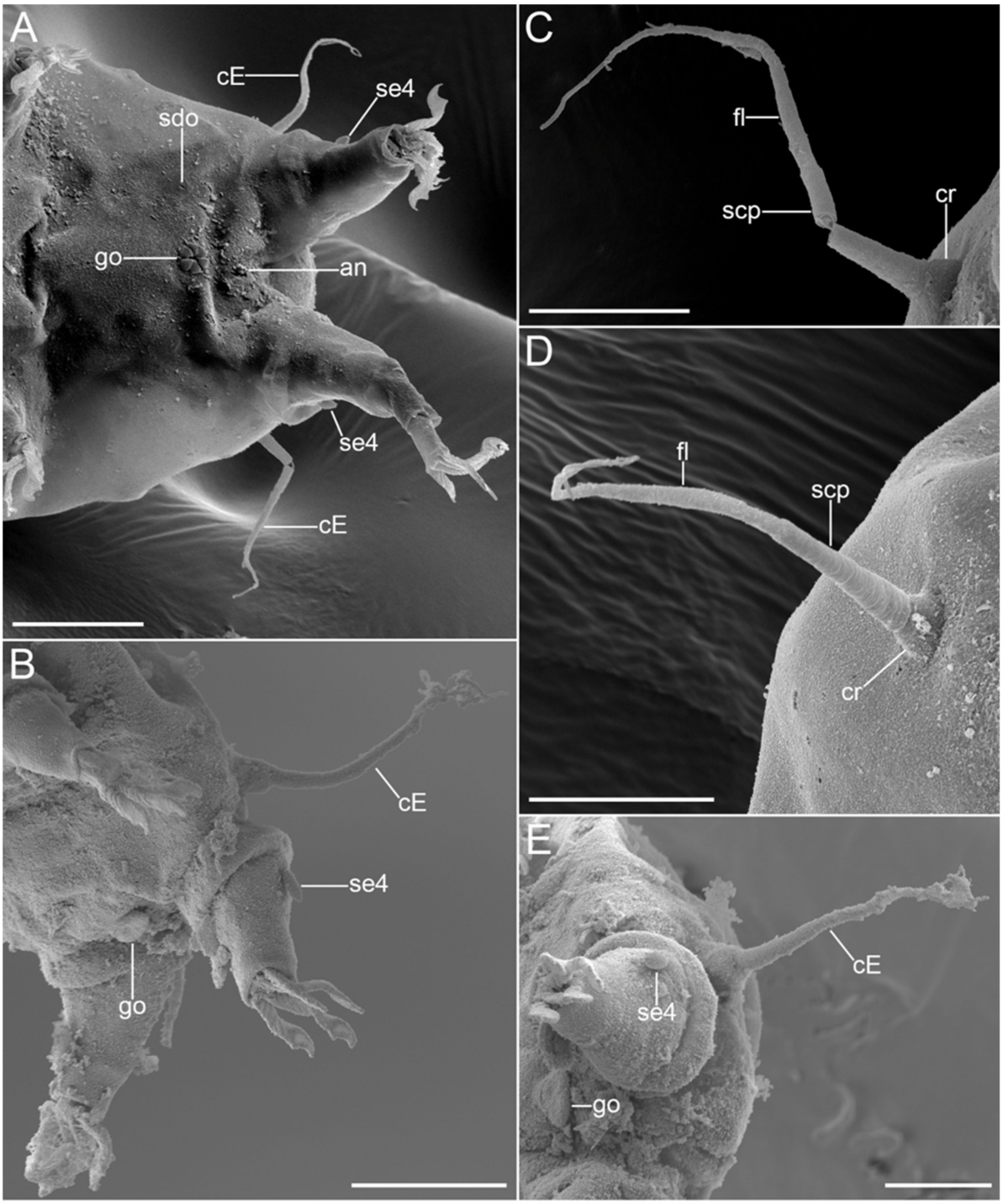

Figure 18. *Moebjergarctus okhotensis* sp. nov. Scanning electron microscopy. (**A**) Caudal region of female; (**B**) Caudal region of male; (**C**,**D**) Cirrus *E*; (**E**) Cirrus *E*, male gonopore and sensory organ legs IV. The letter designations are as follows: cE—cirrus *E*; cr—cirrophore; fl—flagellum; go—gonopore; scp—scapus; sdo—seminal receptacle duct opening; se4—sensory organ legs IV. Scale bars: (**A**)—20 μm; (**B**)—50 μm; (**C**–**E**)—10 μm.

Each of the telescopic legs has a coxa, femur, tibia, and tarsus. The tibia can be retracted into the femur. The tarsus bears four corkscrew-shaped digits, each with simple crescent-shaped claws surrounded by membranous sheaths (Figures 11C,D and 16C–E). The digits on the first three pairs of legs are shorter than on legs IV; on each leg, the internal digits are

longer than the external ones (8.9 and 7.1 µm on legs I–III; 12.7 and 10.2 µm for the internal and external digits, respectively, on legs IV).

The mouth opening is located on top of the conical head. Stylets and stylet supports are not clearly recognizable. The buccal tube is 44.0 µm long. The pharyngeal bulb is ca. 15.1 µm in diameter and has three indistinct placoids. The female gonopore (10.3 µm in diameter) consists of six rosette cells (Figures 15C,D,F, 18A and 20A). The seminal receptacles are elongated and continue into long S-shaped seminal receptacle ducts (Figures 19 and 20A). The triangular male gonopore is circular, with two slightly protruding internal folds (Figures 18B,E and 20B).

A caudodorsal bulge is present at the posterior end of the body, protruding 5.4 µm above the body surface, and is covered by cuticular thickening. The size of the bulge and the thickness of the cuticle vary between individuals (Figure 21, Table 3). The function of this bulge remains unknown.

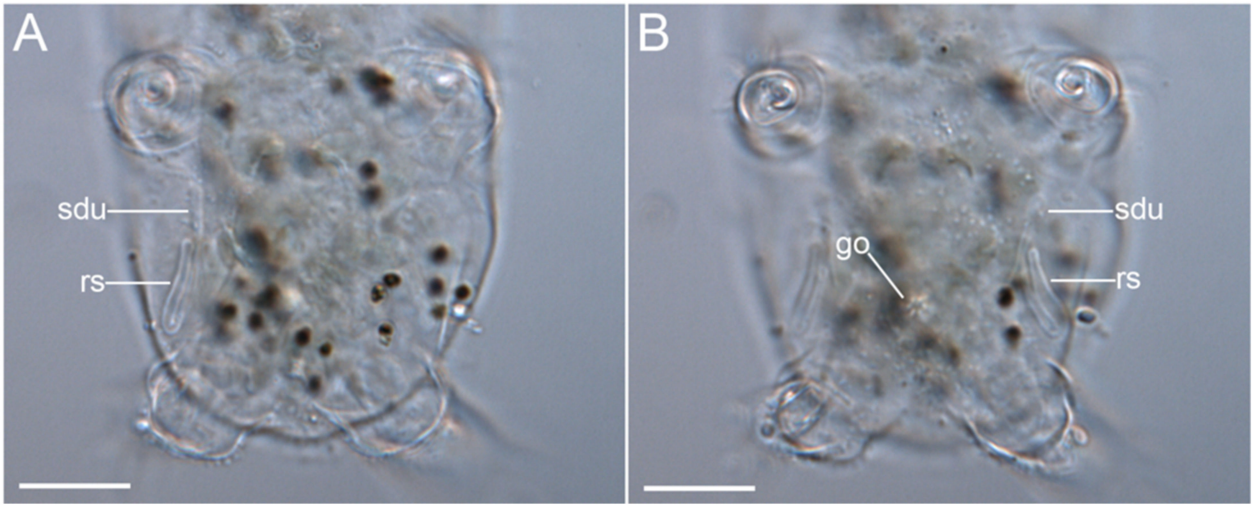

Figure 19. *Moebjergarctus okhotensis* sp. nov. (**A**,**B**) Female gonopore, seminal receptacle, and seminal receptacle duct in the paratype. The letter designations are as follows: go—gonopore; rs—seminal receptacle; sdu—seminal receptacle duct. Scale bars: 20 µm.

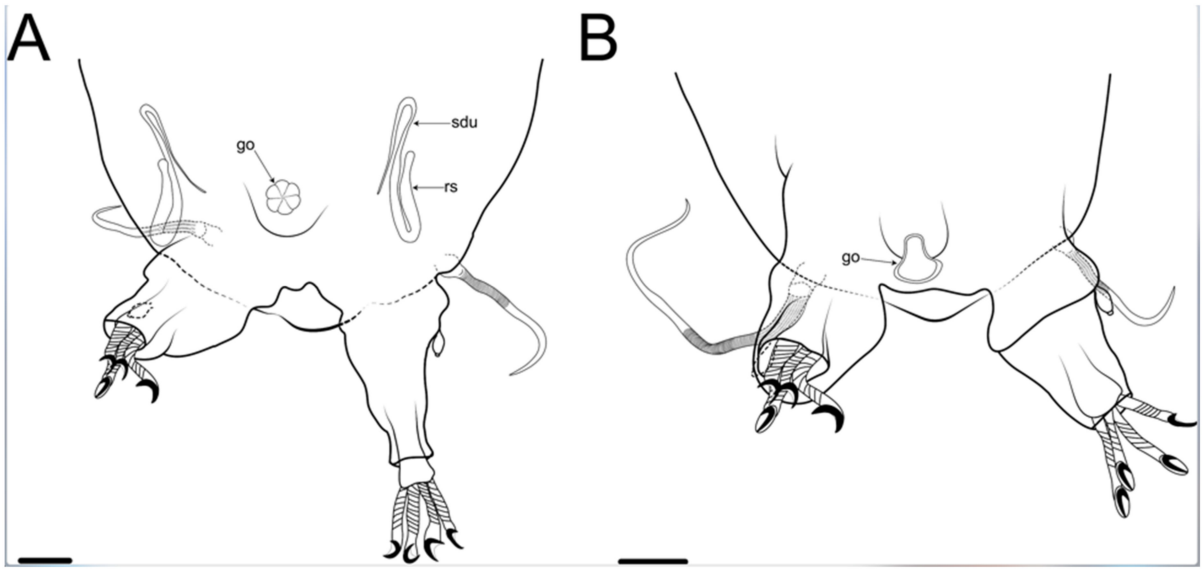

Figure 20. *Moebjergarctus okhotensis* sp. nov. (**A**) Schematic drawing of the female genital structures; (**B**) Schematic drawing of the male genital structures. Abbreviations: go—gonopore; rs—seminal receptacle; sdu—seminal receptacle duct. Scale bar: 20 µm.

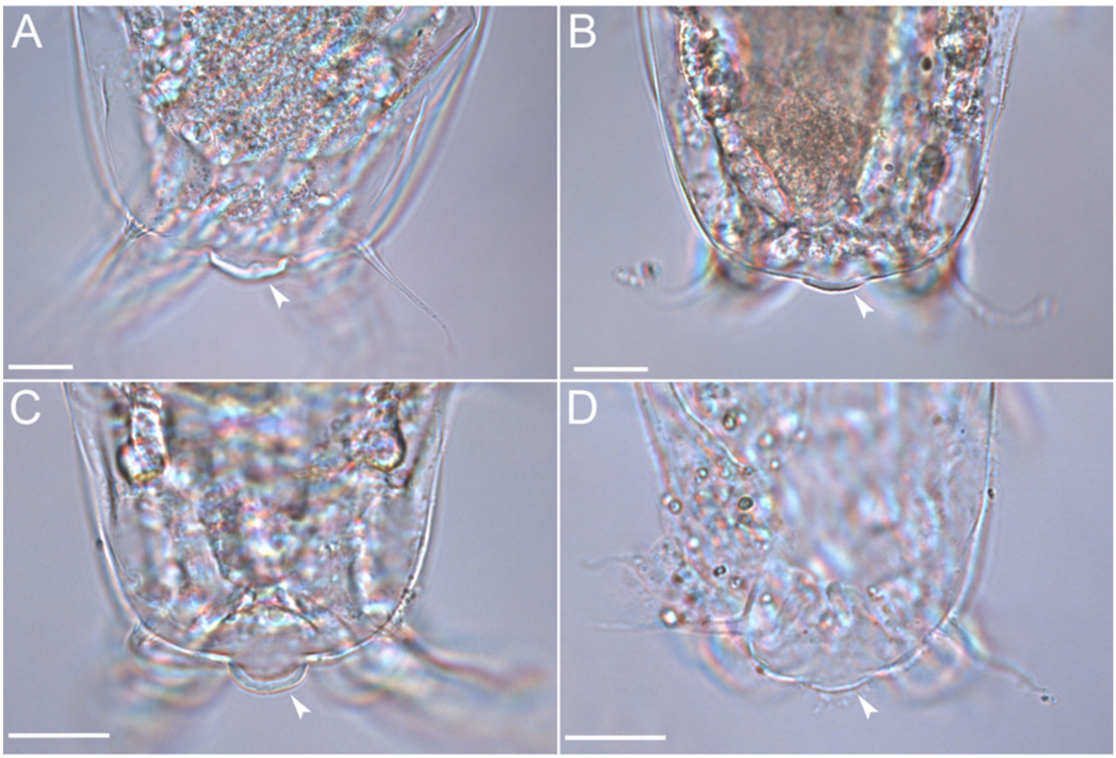

Figure 21. *Moebjergarctus okhotensis* sp. nov. (**A**–**D**) Caudal regions of different paratypes, with the caudodorsal bulge covered by a crescent-shaped cuticular thickening (arrows). Scale bar: 20 μm.

3.2.7. Differential Diagnosis

Based on the morphology of the primary and secondary clavae, cephalic cirri, corkscrew-shaped digits, and crescent-shaped claws, the new species was assigned to the genus *Moebjergarctus*. The new species is very similar to the two existing species *Moe. manganis* Bussau, 1992 [23], and *Moe. clarionclippertonensis* Bai, Wang, Zhou, Lin, Meng, Fontoura, 2020 [12]. However, *Moebjergarctus okhotensis* sp. nov. differs from:

Moe. manganis by cephalic cirri with the long smooth portion of the scapus and the annulated scapus only in the basal portion. In addition, all leg sensory organs are described as spines in *Moe. manganis*, while in *Moebjergarctus okhotensis* sp. nov. is divided into a cirrophore, a scapus, and a short tubular tip. However, it is possible that this character may have been overlooked by Bussau [23] during the light microscopy examination.

Moe. clarionclippertonensis by the presence of a triangular seminal receptacle duct pouch in the female reproductive system and a cuticular platelet in the structure of the male gonopore. In addition, there are differences in the sizes of some structures: the median cirrus, the leg VI sensory organs, the buccal canal, and the external and internal digits on all pairs of legs in the new species are much smaller than in *Moe. clarionclippertonensis* in all individuals.

The caudodorsal bulge described for *Moe. clarionclippertonensis* is also present in *Moebjergarctus okhotensis* sp. nov. The original description of *Moe. manganis* does not mention the caudodorsal bulge, but the figure shows the presence of a similar structure [23].

3.3. Taxonomy

Family Styraconyxidae Kristensen and Renaud-Mornant, 1983 (emended by Fujimoto et al., 2017)

Genus *Angursa* Pollock, 1979

Angursa cf. *bicuspis*

(Figures 22–29, Table 4)

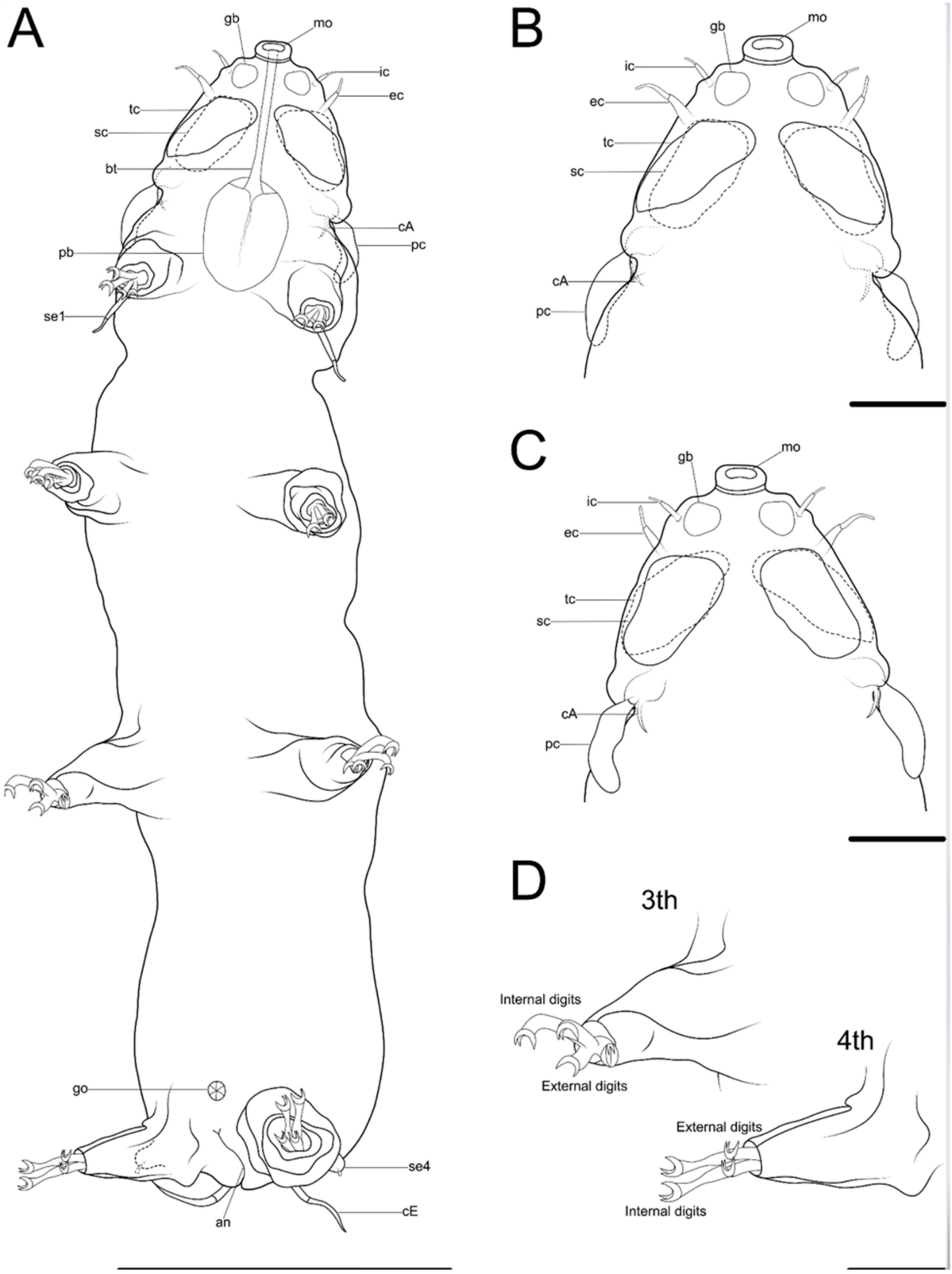

Figure 22. Drawing of *Angursa* cf. *bicuspis*. (**A**) Habitus, ventral view; (**B**) Ventral view of the head; (**C**) Dorsal view of the head; (**D**) Legs III and IV with digits. The letter designations are as follows: an—anus; bt—buccal tube; cA—lateral cirrus *A*; cE—cirrus *E*; ec—external cirrus; gb—globular body; go—gonopore; ic—internal cirrus; mo—mouth opening; pb—pharyngeal bulb; pc—primary clava; sc—secondary clava; se1—sensory organ legs I; se4—sensory organ legs IV; tc—tertiary clavae. Scale bars: (**A**)—50 μm; (**B**–**D**)—10 μm.

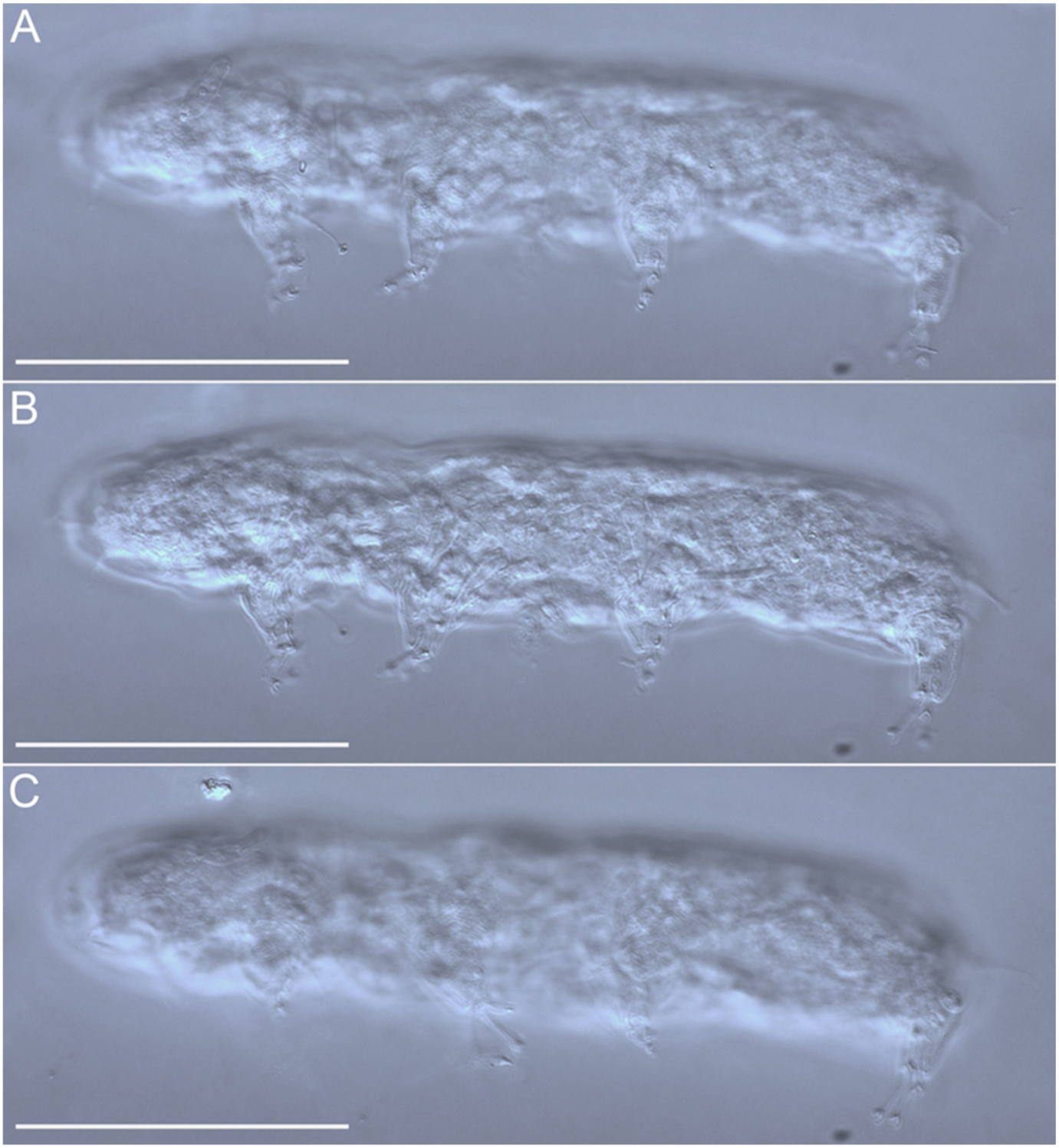

Figure 23. *Angursa* cf. *bicuspis*. (**A**–**C**) Habitus, lateral view. Scale bars: 50 μm.

3.3.1. Material Examined

Two female specimens collected at station SB11 (47°12.0′ N, 149°37.0′ E, 3366 m depth) and four male specimens collected at station SB4 (45°36.3′ N, 146°23.1′ E, 3206 m depth).

Other material: two SEM specimens.

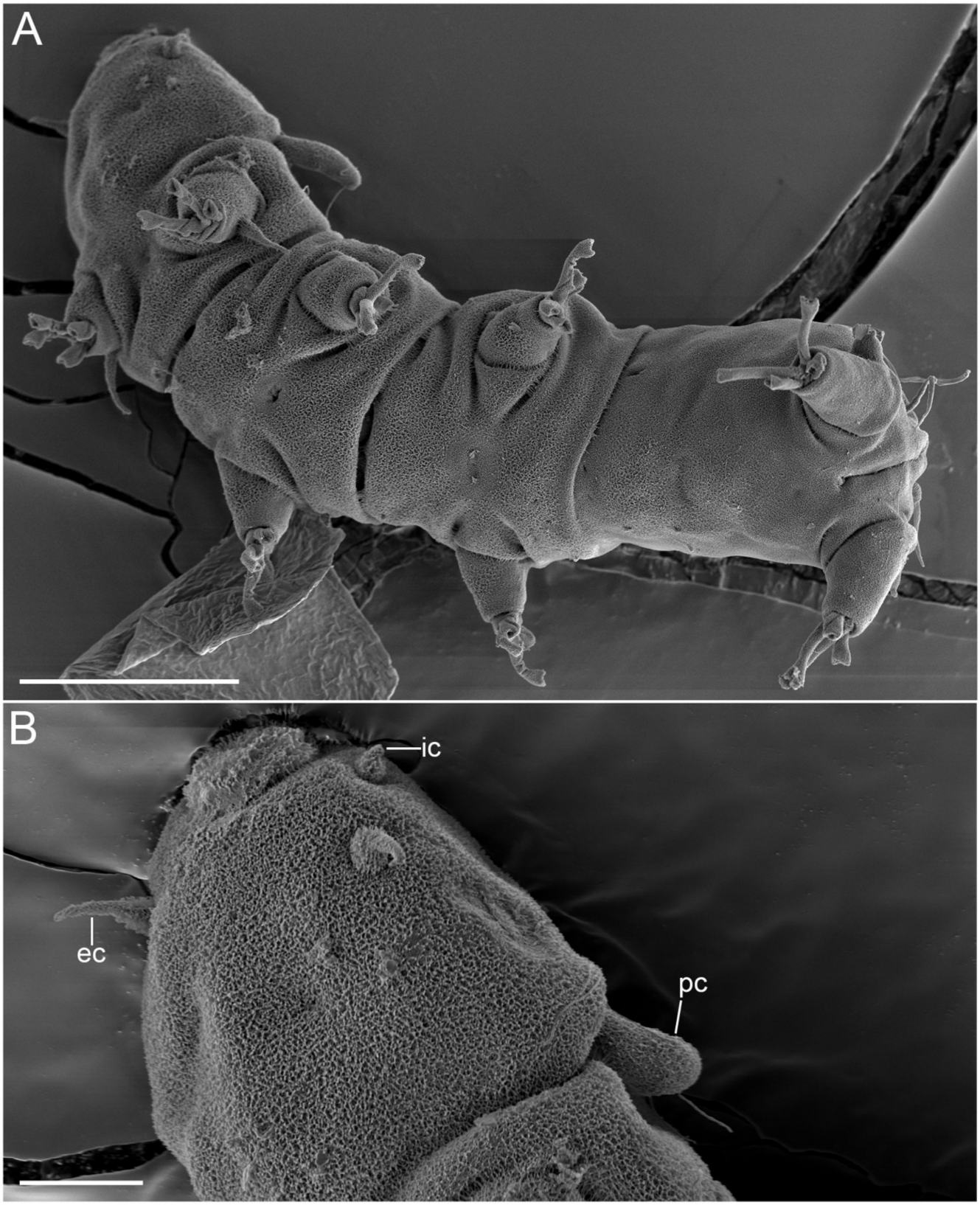

Figure 24. *Angursa* cf. *bicuspis.* Scanning electron microscopy. (**A**) Habitus, ventral view; (**B**) Head with primary clavae and cephalic cirri. The letter designations are as follows: ec—external cirrus; ic—internal cirrus; pc—primary clava. Scale bars: (**A**)—20 μm; (**B**)—5 μm.

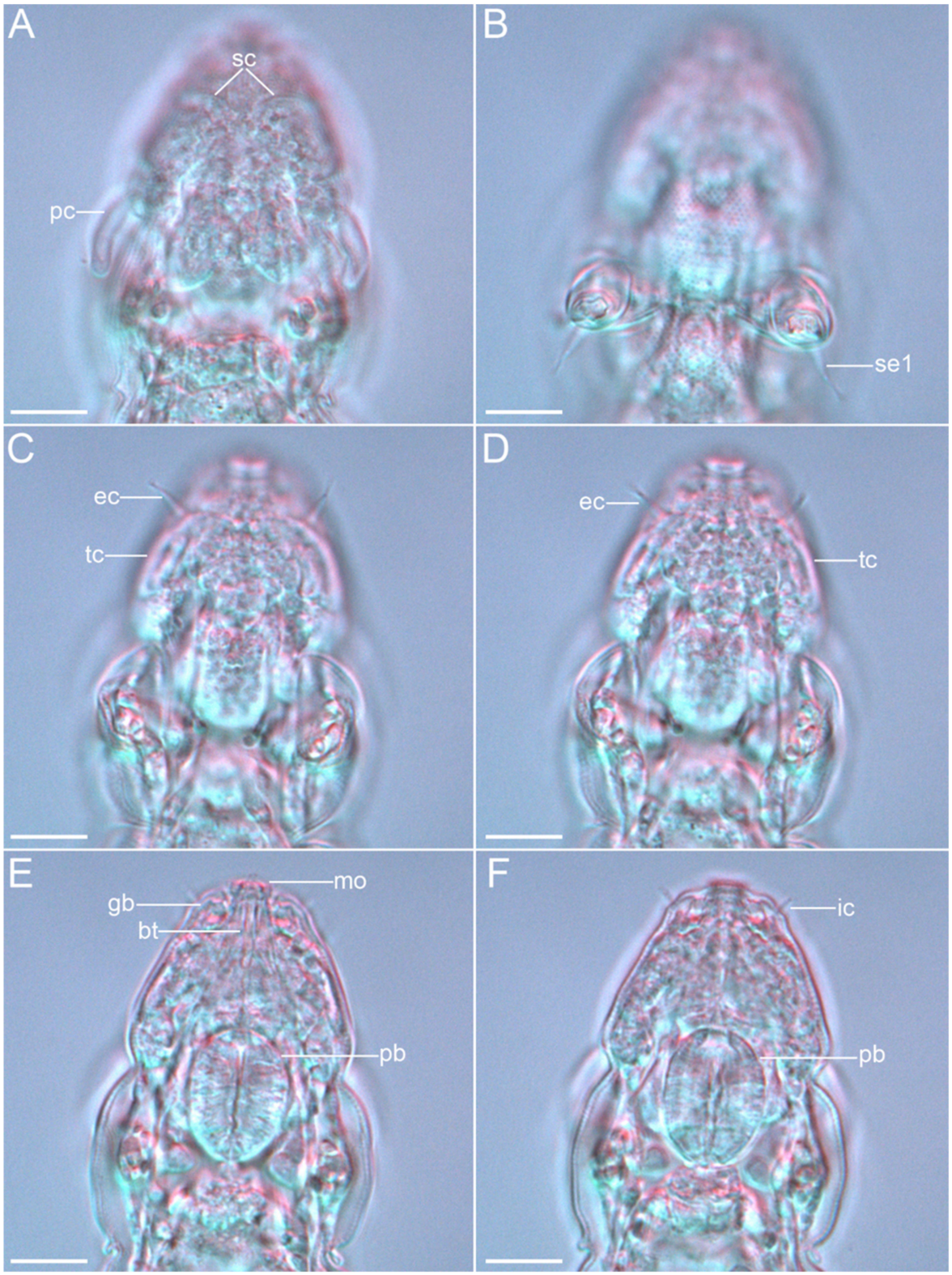

Figure 25. *Angursa* cf. *bicuspis.* Cephalic region of female. (**A**) Dorsal view showing the primary and secondary clavae; (**B**) Leg I sensory organs, ventral view; (**C**,**D**) Ventral view showing the external cirri and tertiary clavae; (**E**,**F**) Ventral view showing the internal cirri, globular body, and mouth opening with buccal tube and pharyngeal bulbus. The letter designations are as follows: bt—buccal tube; ec—external cirrus; gb—globular body; ic—internal cirrus; mo—mouth opening; pb—pharyngeal bulb; pc—primary clava; sc—secondary clava; se1—sensory organ legs I; tc—tertiary clavae. Scale bars: 10 μm.

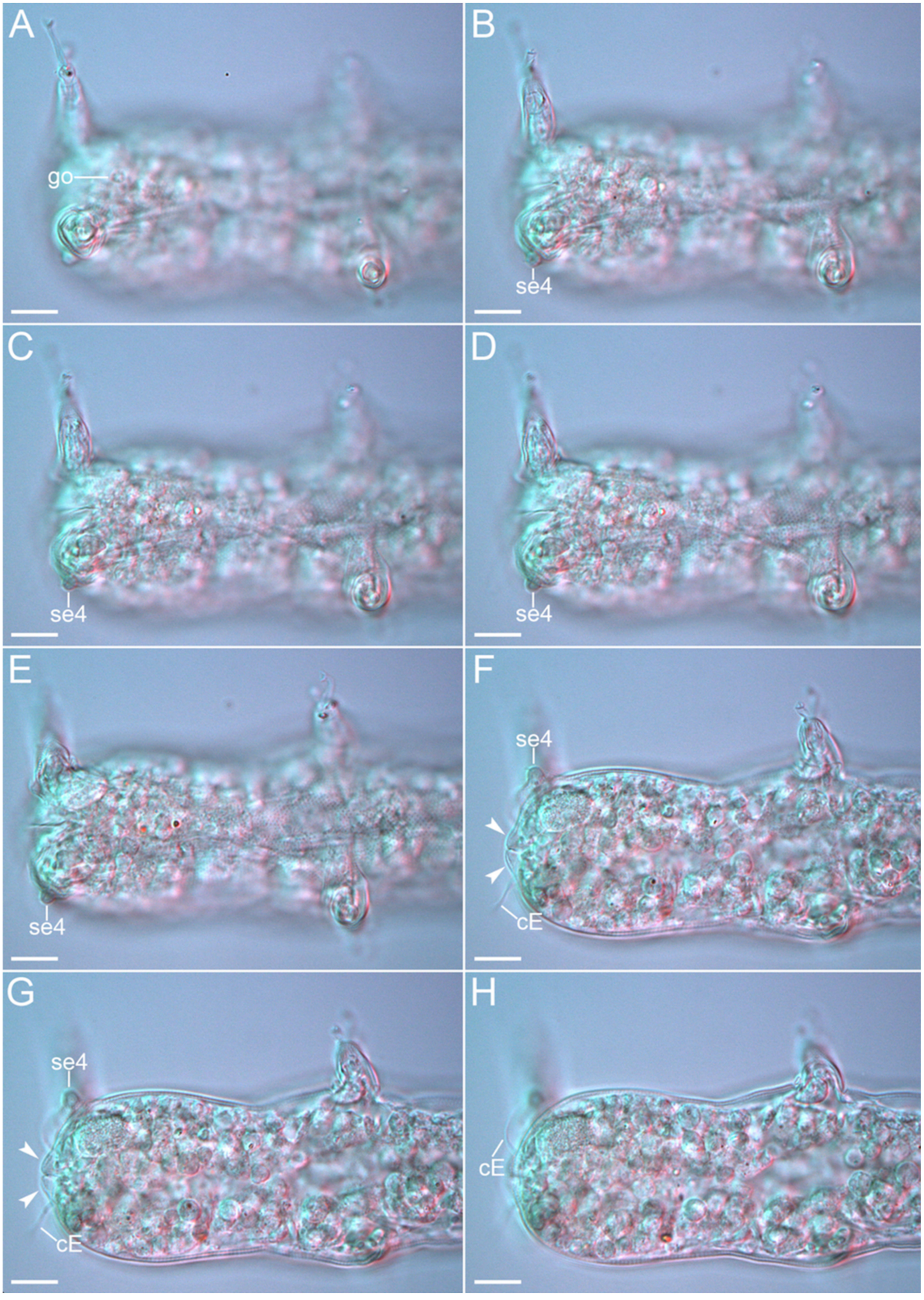

Figure 26. *Angursa* cf. *bicuspis.* Caudal region of female. (**A**–**D**) Ventral view showing the female gonopore and legs IV sensory organ; (**E**–**H**) Dorsal view showing the legs IV sensory organs, cirrus *E*, and anal papillae (arrows). The letter designations are as follows: cE—cirrus *E*; go—gonopore; se4—sensory organ legs IV. Scale bars: 10 μm.

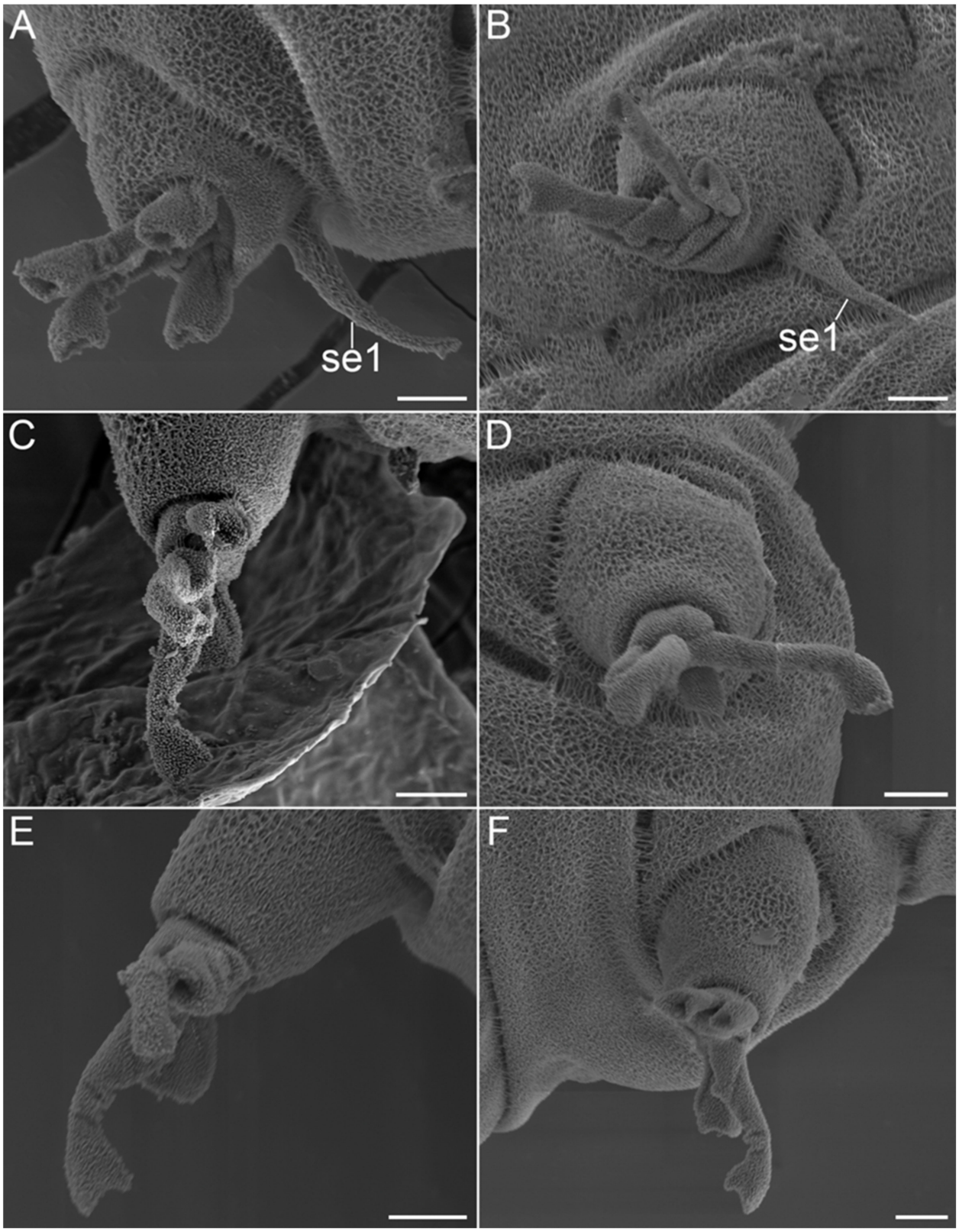

Figure 27. *Angursa* cf. *bicuspis.* Scanning electron microscopy. (**A**) Leg I (right) with sensory organ; (**B**) Leg I (left) with sensory organ; (**C**) Leg II (right); (**D**) Leg II (left); (**E**) Leg III (right); (**F**) Leg III (left). The letter designations are as follows: se1—sensory organ legs I. Scale bars: 2 μm.

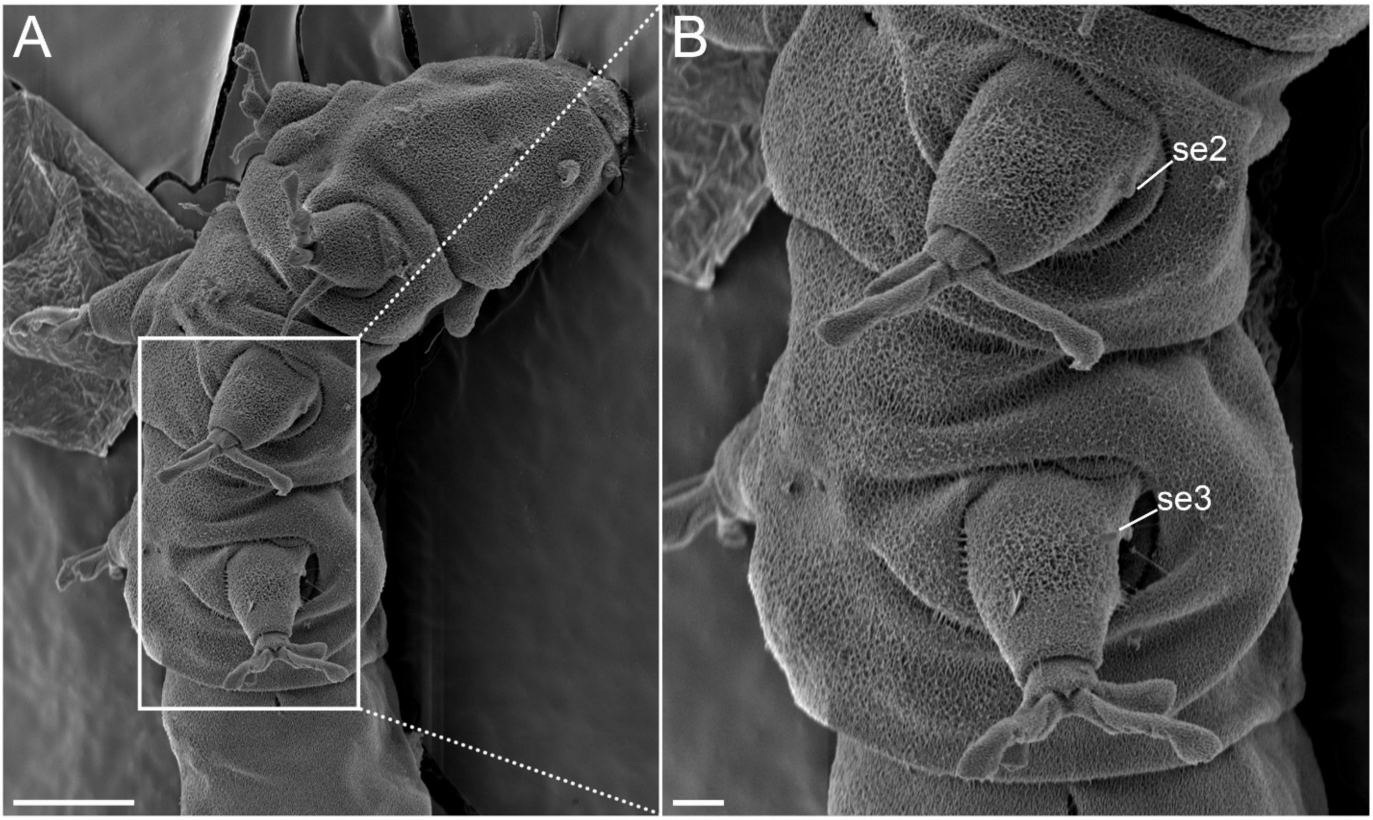

Figure 28. *Angursa* cf. *bicuspis.* Scanning electron microscopy. (**A**,**B**) Sensory organs on legs II and III. The letter designations are as follows: se2–3—sensory organ legs II–III. Scale bars: (**A**)—10 μm; (**B**)—2 μm.

Table 4. Measurements (in μm) of *Angursa* cf. *bicuspis* type series. Body width was measured between legs III and IV; ?—trait not measurable.

Character	Specimen 1, Female	Specimen 2, Female	Specimen 3, Male	Specimen 4, Male	Specimen 5, Male	Specimen 6, Male
Body length	159.1	177.7	147.8	137.7	145.9	179.3
Body width	38.4	?	42.7	43.1	40.3	?
Head width	29.4	?	33.7	35.5	33.3	?
Internal cirri	3.2	2.4	?	4.4	?	?
External cirri	5.8	8.0	7.0	6.4	7.4	5.1
Median cirrus	?	?	?	?		
Cirri *A*	4.3	3.5	?	7.7	7.9	4.5
Primary clava	10.3	12.3	11.1	10.5	9.8	12.8
Secondary clava	11.4	10.6	?	?	?	?
Tertiary clava	10.3	10.6	?	?	?	?
Distance between secondary clavae	2.8	?	?	?	?	?
Cirri *E*	12.8	12.4	14.1	13.8	?	14.7
Sensory organ leg I	12.1	12.2	?	7.6	?	12.1
Sensory organ leg II	?	?	?	?	?	?
Sensory organ leg III	?	?	?	?	?	?
Papillae of legs IV	3.2	4.0	4.3	4.2	?	3.1

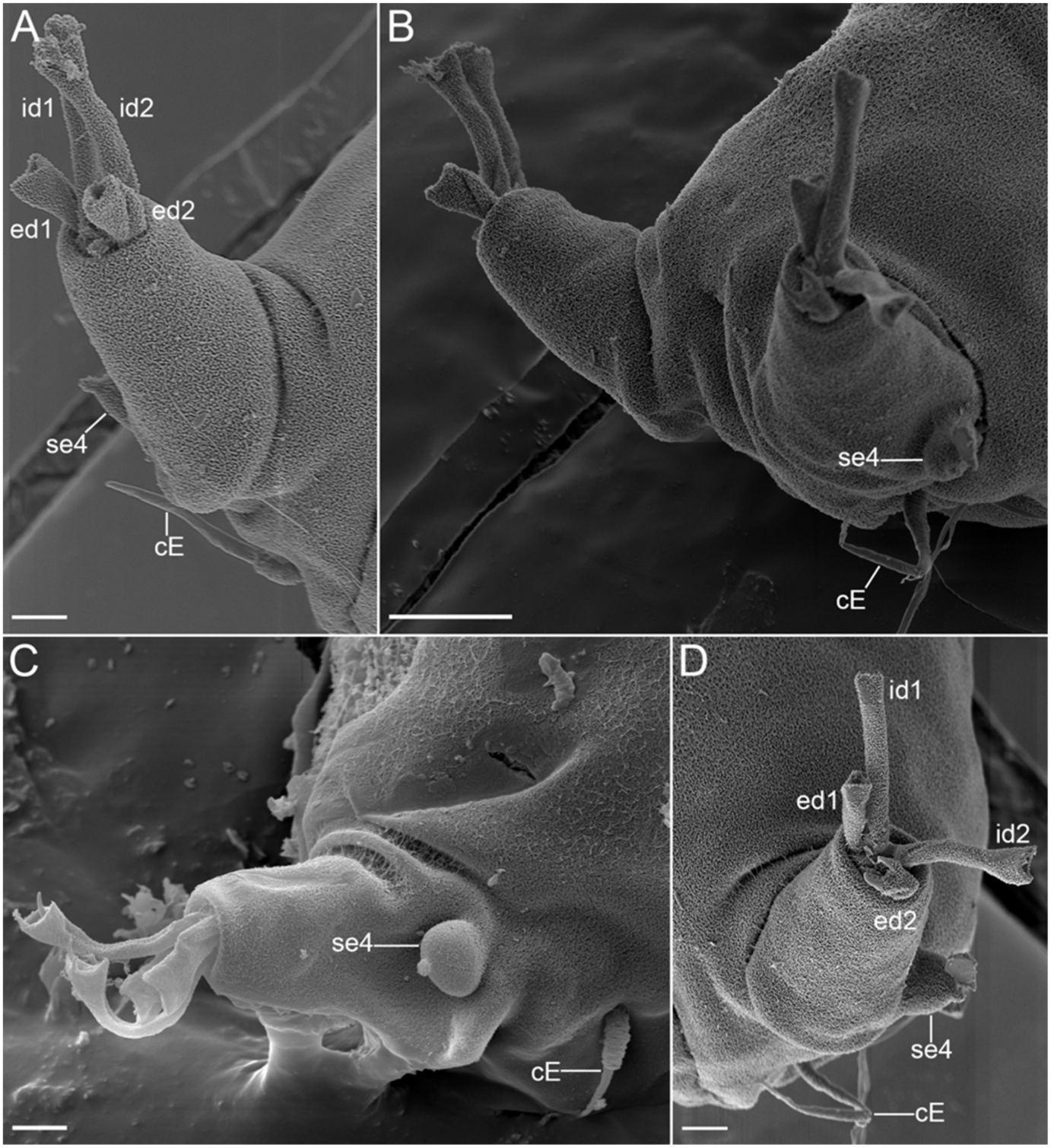

Figure 29. *Angursa* cf. *bicuspis*. Scanning electron microscopy. (**A**) Leg IV (right) with digits and sensory organs; (**B**) Legs IV with sensory organs; (**C**,**D**) Leg IV (left) with digits and sensory organs. The letter designations are as follows: cE—cirrus *E*; ed1 and ed2—external digits; id1 and id2—internal digits; se4—sensory organ legs IV. Scale bars: (**A**,**C**,**D**)—2 μm; (**B**)—10 μm.

3.3.2. Morphological Comments

Specimens have elongated slender bodies. Head had weak neck constriction anterior of legs I bearing sensory organs: paired internal cirri (2.4–4.4 μm long), paired external cirri

(5.1–8.0 µm long), paired lateral cirri *A* (3.5–7.7 µm long), paired primary clavae (9.8–12.8 µm long), paired secondary clavae (10.6–11.4 µm long and 6.0 µm wide), and paired tertiary clavae (10.3–10.6 µm long and 7.1 µm wide) (Figures 22B,C, 24B,C and 25). The median cirrus was not found and was apparently absent. External cirri are inserted ventrally; internal cirri are inserted dorsally on the anterior margin of the body, each consisting of a scapus and a distal flagellar part with a blunt tip (Figure 22B,C). Lateral cirri *A* and club-shaped primary clavae are positioned dorsolaterally on a slightly raised pedestal (Figures 22C and 25A). Secondary clavae are flat, located dorsally, and situated close to one another (2.8 µm between clavae) (Figures 22C and 25A). Tertiary clavae are flat and located ventrally (Figures 22B and 25C,D). The secondary and tertiary clavae do not have any lobes. The mouth opening is located at the front end of the head and directed anteriorly. A paired globular body (1.9 µm in diameter) fringing the mouth is present (Figure 22B,C). Stylets and stylet supports are not visible. A pair of cirri *E* (12.8–14.7 µm long) is located dorsally on the coxae of legs IV (Figure 29). Each simple cirrus *E* consists of a cirrophore, a short scapus, and a long flagellar part. The scapus is annulated but is visible only in SEM (Figure 29). Each telescopic leg consists of a coxa, femur, tibia, and tarsus. The tibia can be retracted into the femur. Each tarsus bears four digits ending in claws with two diverging points (Figures 22D, 27 and 29). Legs I have a spine-shaped sensory organ (7.6–12.2 µm long) present on the femur, consisting of two parts: proximal and distal with a blunt tip (Figures 25B and 27A,B). The sensory organs on legs II and III were not visible under light microscopy but were present on the femur in SEM photographs as very short blunt-ended spines (Figure 28). The sensory organ on leg IV is hemispherical, 3.1–4.2 µm in length, and 3 µm in diameter, with a short apical tip (Figure 29). The digits of the first three pairs of legs are shorter than the digits on legs IV; the internal digits are always longer than the external digits. The female gonopore (about 3.5 µm in diameter) consists of six rosette-like cells located 3 µm anterior of the anus (Figure 26A). Seminal receptacles and genital ducts were not visible. The anus area is flanked by two 2.5 µm cuticular papillae (Figure 26C).

In general, all our specimens match the description of *Angursa bicuspis* Pollock, 1979 [24,25]. The presence of sensory organs on legs I and II may have been overlooked by Pollock [24] since this trait can only be seen under SEM. Similarly, the slightly raised pedestal on which the primary clavae and lateral cirri are located is poorly distinguishable. Our specimens have anal papillae, but the expression of this character varies between individuals and therefore should be used as a distinguishing trait with caution. At the same time, it should be noted that the original description of *Ang. bicuspis* has no information about the structure of the secondary and tertiary clavae.

4. Discussion

An analysis of the results of the four deep-sea expeditions to the NWPO has shown a rather high frequency of the occurrence of tardigrades (ca. 50%) found at depths from 1473 to 9540 m. The factors responsible for the distribution of deep-sea tardigrades remain unclear. However, there is evidence that a higher diversity has been registered in medium to coarse sediments, especially in carbonate sands deposited in shallow environments [26–28]. Data analyses indicate the high richness and peculiarity of marine tardigrade fauna [11,28–32]. In general, the distribution pattern of tardigrades in the NWPO is mosaic. This type of distribution is often reported for marine tardigrades [28,33,34].

All three genera found by us were previously registered in other deep-sea ecosystems. Up to now, only 51 tardigrades species (along with those presented in this paper) from 23 genera have been reported deeper than 200 m [3,5]. Some of these species have only been recorded in deep-sea bottom sediments, some have also been found in shallow subtidal and tidal communities [5]. Representatives of nine genera were found only deeper than 200 m: *Bathyechiniscus* Steiner, 1926; *Clavarctus* Renaud-Mornant, 1983; *Coronarctus* (with the exception of *Cor. neptunus*, found at depths of 150–1300 m); *Exoclavarctus* Renaud-Mornant, 1983; *Euclavarctus* Renaud-Mornant, 1975; *Moebjergarctus*; *Ligiarctus* Renaud-Mornant, 1982; *Parmursa* Renaud-Mornant, 1984; and *Proclavarctus* Renaud-Mornant, 1983 [35–39]. Our

finding of new *Coronarctus* and *Moebjergarctus* deep-sea species may be an additional sign of the presence of specialized deep-sea tardigrade fauna. At the same time, the analysis of the distribution patterns of marine tardigrades along geographic gradients is currently severely limited by the poor knowledge of this taxon [40]. Undersampling is a true problem in marine tardigrade research, for which many understudied and unstudied areas remain [40,41].

The *Coronarctus* has been recorded from the Pacific Ocean for the first time; previously, representatives of the genus were found only in the Atlantic and Indian Oceans [5,12,21,22]. *Moebjergarctus okhotensis* sp. nov. is the third known species of the genus, and all representatives have been recorded from deep-sea communities of the Pacific Ocean [11,23]. The spatial distribution of the species varied significantly: *Cor. sonne* sp. nov. occurred only on the Pacific abyssal plain adjacent to the Kuril–Kamchatka Trench, while *Moe. okhotensis* sp. nov. occurred only at stations in the Kuril Basin in the Sea of Okhotsk.

In contrast to the two genera discussed above, representatives of *Angursa* are characterized by very wide geographic and bathymetric distribution gradients. Species of this genus are found in the Atlantic, Pacific, and Southern oceans in both intertidal and deep-sea habitats. This genus is characterized by both exclusively deep-sea species (*Ang. abyssalis*, Ang. lanceolata, Ang. capsula, Ang. antarctica, and Ang. seisuimaruae) and those with very wide distributions and occurring at various depths, including the littoral (*Ang. lingua* and Ang. bicuspis) [5,14,23,24,42,43].

It should particularly be noted that the identification of species of the genus *Angursa* based solely on morphological characters, which can often be poorly distinguishable, is a major challenge. For this reason, we identified samples from the Sea of Japan and stations in the Pacific Ocean only to the genus level. Moreover, the original descriptions of several species do not provide information about some important characteristics. In particular, the description of *Ang. bicuspis* lacks information on the structures of the secondary and tertiary clavae [10,24]. Thus, an assumption can be made that, in several cases, data on the very wide distribution of species and occurrence in both intertidal and abyssal zones may be associated with incorrect species identification. A wider use of molecular phylogenetic methods may address this problem in the future.

Author Contributions: A.A.S.: conceptualization, data curation, formal analysis, methodology, investigation, validation, visualization, and writing—original draft; A.S.M.: conceptualization, data curation, visualization, and writing—review and editing; P.M.A.: data curation and writing—review and editing; V.V.M.: conceptualization, data curation, formal analysis, methodology, investigation, validation, funding acquisition, project administration, and writing—review and editing. All authors have read and agreed to the published version of the manuscript.

Funding: The study was funded by the Ministry of Science and Higher Education of the Russian Federation (grant 13.1902.21.0012/2, contract No. 075-15-2020-796).

Institutional Review Board Statement: Not applicable.

Data Availability Statement: Not applicable.

Acknowledgments: The scanning electron microscopy (SEM) investigations were carried out at the A.V. Zhirmunsky National Scientific Centre of Marine Biology FEB RAS. The authors are grateful to D.V. Fomin for assistance with the SEM facilities. The light microscopy examinations were carried out in the Laboratory of Ecology and Evolutionary Biology of Aquatic Organisms of the Far Eastern Federal University. We are very grateful to A. Brandt (Senckenberg Research Institute and Natural History Museum, and Goethe University Frankfurt, Frankfurt, Germany) and to M.V. Malyutina (NSCMB FEB RAS) for the invitation to join the international project and the deep-sea expeditions. We thank the crews of the RV *Sonne* and RV *Akademik M.A. Lavrentyev* and the research teams of the expeditions for their assistance and support on board.

Conflicts of Interest: The authors declare no conflict of interest.

References

1. Nelson, D.R.; Bartels, P.J.; Guil, N. Tardigrade ecology. In *Water Bears: The Biology of Tardigrades*; Schill, R.O., Ed.; Springer International Publishing: Cham, Switzerland, 2018; pp. 163–210. [CrossRef]
2. Hengherr, S.; Schill, R.O. Environmental adaptations: Cryobiosis. In *Water Bears: The Biology of Tardigrades*; Schill, R.O., Ed.; Springer International Publishing: Cham, Switzerland, 2018; pp. 295–310. [CrossRef]
3. Degma, P.; Bertolani, R.; Guidetti, R. Actual Checklist of Tardigrada Species, (41st Edition: 12-05-2022); 2009–2022. Available online: http://www.evozoo.unimore.it/site/home/tardigrade-tools/documento1080026927.html (accessed on 15 September 2022).
4. Mcinnes, S.J.; Jørgensen, A.; Michalczyk, Ł. 20 Years of Zootaxa: Tardigrada (Ecdysozoa: Panarthropoda). *Zootaxa* **2021**, *4979*, 23–24. [CrossRef] [PubMed]
5. Kaczmarek, L.; Bartels, P.J.; Roszkowska, M.; Nelson, D.R. The zoogeography of marine Tardigrada. *Zootaxa* **2015**, *4037*, 1–189. [CrossRef] [PubMed]
6. Schmidt, C.; Sattarova, V.V.; Katrynski, L.; Martínez Arbizu, P. New insights from the deep: Meiofauna in the Kuril-Kamchatka Trench and adjacent abyssal plain. *Prog. Oceanogr.* **2019**, *173*, 192–207. [CrossRef]
7. Fontoura, P.; Bartels, P.J.; Jørgensen, A.; Kristensen, R.M.; Hansen, J.G. A dichotomous key to the genera of the marine heterotardigrades (Tardigrada). *Zootaxa* **2017**, *4294*, 1–45. [CrossRef]
8. Topstad, L.; Guidetti, R.; Majaneva, M.; Ekrem, T. Multi-marker DNA metabarcoding reflects tardigrade diversity in different habitats. *Genome* **2021**, *64*, 217–231. [CrossRef]
9. Bartels, P.J.; Apodaca, J.J.; Mora, C.; Nelson, D.R. A global biodiversity estimate of a poorly known taxon: Phylum Tardigrada. *Zool. J. Linn. Soc.* **2016**, *178*, 730–736. [CrossRef]
10. Tchesunov, A.V. A new tardigrade species of the genus *Neostygarctus* Grimaldi de Zio et al., 1982 (Tardigrada, Arthrotardigrada) from the Great Meteor Seamount, Northeast Atlantic. *Eur. J. Taxon.* **2018**, *479*, 1–17. [CrossRef]
11. Bai, L.; Wang, X.; Zhou, Y.; Lin, S.; Meng, F.; Fontoura, P. *Moebjergarctus clarionclippertonensis*, a new abyssal tardigrade (Arthrotardigrada, Halechiniscidae, Euclavarctinae) from the Clarion-Clipperton Fracture Zone, North-East Pacific. *Zootaxa* **2020**, *4755*, 561–575. [CrossRef]
12. Gomes-Júnior, E.; Santos, É.; da Rocha, C.M.C.; Santos, P.J.P.; Fontoura, P. The deep-sea genus *Coronarctus* (Tardigrada, Arthrotardigrada) in Brazil, south-western Atlantic Ocean, with the description of three new species. *Diversity* **2020**, *12*, 63. [CrossRef]
13. Hansen, J.G.; Kristensen, R.M. A new genus and five new species of the subfamily Florarctinae (Tardigrada, Arthrotardigrada). *Eur. J. Taxon.* **2021**, *762*, 149–184. [CrossRef]
14. Fujimoto, S.; Hansen, J.G. Revision of Angursa (Arthrotardigrada: Styraconyxidae) with the description of a new species from Japan. *Eur. J. Taxon.* **2019**, *2019*, 1–19. [CrossRef]
15. Schmidt, C.; Martínez Arbizu, P. Unexpectedly higher metazoan meiofauna abundances in the Kuril–Kamchatka Trench compared to the adjacent abyssal plains. *Deep Sea Res. Part II Top. Stud. Oceanogr.* **2015**, *111*, 60–75. [CrossRef]
16. Brandt, A.; Brix, S.; Riehl, T.; Malyutina, M. Biodiversity and biogeography of the abyssal and hadal Kuril-Kamchatka trench and adjacent NW Pacific deep-sea regions. *Prog. Oceanogr.* **2020**, *181*, 102232. [CrossRef]
17. McIntyre, A.D.; Warwick, R.M. Meiofauna techniques. In *Methods for the Study of Marine Benthos*; Blackwell: Oxford, UK, 1984.
18. Guil, N.; Jørgensen, A.; Kristensen, R. An upgraded comprehensive multilocus phylogeny of the Tardigrada tree of life. *Zool. Scr.* **2019**, *48*, 120–137. [CrossRef]
19. Møbjerg, N.; Jørgensen, A.; Kristensen, R.M.; Cardoso Neves, R.A. Morphology and functional anatomy. In *Water Bears: The Biology of Tardigrades*; Schill, R.O., Ed.; Springer International Publishing: Cham, Switzerland, 2018; pp. 57–94. [CrossRef]
20. Perry, E.; Miller, W.R.; Kaczmarek, Ł. Recommended abbreviations for the names of genera of the phylum Tardigrada. *Zootaxa* **2019**, *4608*, 145–154. [CrossRef]
21. Renaud-Mornant, J. Bathyal and abyssal Coronarctidae (Tardigrada), description of new species and phylogenetical significance. In *Biology of Tardigrades. Selected Symposia and Monographs U.Z.I*; Bertolani, R., Ed.; Mucchi Editore: Modena, Italy, 1987; Volume 1, pp. 93–101.
22. Romano, F., III; Gallo, M.; D'Addabbo, R.; Accogli, G.; Bagueley, J.; Montagna, P. Deep-sea tardigrades in the northern Gulf of Mexico with a description of a new species of Coronarctidae (Tardigrada: Arthrotardigrada), *Coronarctus mexicus*. *J. Zool. Syst. Evol. Res.* **2011**, *49*, 48–52. [CrossRef]
23. Bussau, C. New deep-sea Tardigrada (Arthrotardigrada, Halechiniscidae) from a manganese nodule area of the Eastern South Pacific. *Zool. Scr.* **1992**, *21*, 79–92. [CrossRef]
24. Pollock, L.W. *Angursa bicuspis* n. g., n. sp., a new marine arthrotardigrade from the western North Atlantic. *Trans. Am. Microsc. Soc.* **1979**, *98*, 558–562. [CrossRef]
25. Noda, H. Description of a new subspecies of *Angursa biscupis* Pollock (Heterotardigrada, Halechiniscidae) from Tanabe Bay, Japan. *Publ. Seto Mar. Biol. Lab.* **1985**, *30*, 269–276. [CrossRef]
26. Renaud-Mornant, J. Tardigrada. In *Introduction to the Study of Meiofauna*; Higgins, R.P., Thiel, H., Eds.; Smithsonian Institution Press: Washigton, DC, USA, 1988; pp. 357–361.
27. Giere, O. *Meiobenthology: The Microscopic Motile Fauna of Aquatic Sediments*, 2nd ed.; Springer Verlag: Berlin/Heidelberg, Germany, 2009; p. 527. [CrossRef]
28. Hansen, J.G.; Jørgensen, A.; Kristensen, R.M. Preliminary studies of the tardigrade fauna of the Faroe Bank. *Zool. Anzeiger A J. Comp. Zool.* **2001**, *240*, 385–393. [CrossRef]

29. Hansen, J.G. The ongoing investigation of the Faroe Bank tardigrade fauna. In *Proceedings of the BIOFAR Symposium, Tórshavn, Faroe Islands, 24–26 April 2003, North-East Atlantic Marine Benthic Oorganisms in the Faroes—Taxonomy, Distribution and Ecology, Tórshavn, Faroe Islands*; Frøðskapparit Supplementum; Føroya Fróðskaparfelag: Tórshavn, Faroe Islands, 2005; pp. 220–223.
30. Jörgensen, A.; Kristensen, R.M. A New tanarctid Arthrotardigrade with buoyant bodies. *Zool. Anzeiger A J. Comp. Zool.* **2001**, *240*, 425–439. [CrossRef]
31. Hansen, J.G.; D'Addabbo, M.G.; de Zio Grimaldi, S. A Comparison of morphological characters within the genus *Rhomboarctus* (Tardigrada: Heterotardigrada) with the description of two new species. *Zool. Anzeiger A J. Comp. Zool.* **2003**, *242*, 83–96. [CrossRef]
32. Kristensen, R.M.; Sørensen, M.V.; Hansen, J.G.; Zeppilli, D. A New species of *Neostygarctus* (Arthrotardigrada) from the Condor Seamount in the Azores, Northeast Atlantic. *Mar. Biodivers.* **2015**, *45*, 453–467. [CrossRef]
33. Pérez-Pech, W.A.; Hansen, J.G.; Demilio, E.; de Jesús-Navarrete, A.; Mendoza, I.M.; Olivares, A.R.; Vargas-Espositos, A. First records of marine tardigrades of the genus *Coronarctus* (Tardigrada, heterotardigrada, arthrotardigrada) from Mexico. *Check List* **2019**, *16*, 1–7. [CrossRef]
34. Bartels, P.J.; Fontoura, P.; Nelson, D.R. Marine tardigrades of the Bahamas with the description of two new species and updated keys to the species of *Anisonyches* and *Archechiniscus*. *Zootaxa* **2018**, *4420*, 43–70. [CrossRef]
35. Renaud-Mornant, J. Deep-sea tardigrada from the "Meteor" Indian Ocean Expedition. *Meteor Forsch. Reihe D Biol.* **1975**, *21*, 54–61.
36. Renaud-Mornant, J. Tardigrades abyssaux nouveaux de la sous-famille des Euclavarctinae n. subfam (Arthrotardigrada, Halechiniscidae). *Bulletin du Muséum National d'Histoire Naturelle, Section A. Zoologie Biologie et Ecologie Animales* **1983**, *51*, 201–219.
37. Steiner, G. *Bathyechiniscus tetronyx* n. g., n. sp., Ein neuer mariner Tardigrade. Deutsche Sudpolar Expedition, 1901–1903. *Zoology* **1926**, *10*, 479–481.
38. Renaud-Mornant, J. Sous-famille et genre nouveaux de Tardigrades marins (Arthrotardigrada). *Bull. Du Muséum Natl. D'histoire Nat.* **1982**, *4*, 89–94.
39. Renaud-Mornant, J. Halechiniscidae (Heterotardigrada) de la campagne Benthedi, canal du Mozambique. *Bull. Du Muséum Natl. D'histoire Nat.* **1984**, *6*, 67–88.
40. Bartels, P.J.; Fontaneto, D.; Roszkowska, M.; Nelson, D.R.; Kaczmarek, Ł. Latitudinal gradients in body size in marine tardigrades. *Zool. J. Linn. Soc.* **2020**, *188*, 820–838. [CrossRef]
41. Kristensen, R.M.; Mackness, B.S. First record of the marine tardigrade genus Batillipes (Arthrotardigrada: Batillipedidae) from South Australia with a description of a new species. *Rec. South Aust. Mus.* **2000**, *33*, 73–87.
42. Renaud-Mornant, J. Deux nouveaux *Angursa* Pollock, 1979, du domaine abyssal (Tardigrada, Arthrotardigrada). *Tethys* **1981**, *10*, 161–164.
43. Villora-Moreno, S. Deep-sea Tardigrada from South Shetland Islands (Antarctica) with description of *Angursa antarctica* sp. nov. (Arthrotardigrada, Halechiniscidae). *Polar Biol.* **1998**, *19*, 336–341. [CrossRef]